International Telecommunication Union

ITU-R

Radiocommunication Sector of ITU

Recommendation ITU-R P.527-6

(09/2021)

Electrical characteristics of the surface of the Earth

P Series

Radiowave propagation

Foreword

The role of the Radiocommunication Sector is to ensure the rational, equitable, efficient and economical use of the radio-frequency spectrum by all radiocommunication services, including satellite services, and carry out studies without limit of frequency range on the basis of which Recommendations are adopted.

The regulatory and policy functions of the Radiocommunication Sector are performed by World and Regional Radiocommunication Conferences and Radiocommunication Assemblies supported by Study Groups.

Policy on Intellectual Property Right (IPR)

ITU-R policy on IPR is described in the Common Patent Policy for ITU-T/ITU-R/ISO/IEC referenced in Resolution ITU-R 1. Forms to be used for the submission of patent statements and licensing declarations by patent holders are available from http://www.itu.int/ITU-R/go/patents/en where the Guidelines for Implementation of the Common Patent Policy for ITU-T/ITU-R/ISO/IEC and the ITU-R patent information database can also be found.

Series of ITU-R Recommendations

(Also available online at http://www.itu.int/publ/R-REC/en)

Series	Title
BO	Satellite delivery
BR	Recording for production, archival and play-out; film for television
BS	Broadcasting service (sound)
BT	Broadcasting service (television)
F	Fixed service
M	Mobile, radiodetermination, amateur and related satellite services
P	**Radiowave propagation**
RA	Radio astronomy
RS	Remote sensing systems
S	Fixed-satellite service
SA	Space applications and meteorology
SF	Frequency sharing and coordination between fixed-satellite and fixed service systems
SM	Spectrum management
SNG	Satellite news gathering
TF	Time signals and frequency standards emissions
V	Vocabulary and related subjects

Note: *This ITU-R Recommendation was approved in English under the procedure detailed in Resolution ITU-R 1.*

Electronic Publication
Geneva, 2021

RECOMMENDATION ITU-R P.527-6

Electrical characteristics of the surface of the Earth

(1978-1982-1992-2017-2019-2021)

Scope

This Recommendation gives methods to model the electrical characteristics of the surface of the Earth, including pure water, sea water, ice, soil and vegetation cover, for frequencies up to 1 000 GHz, in a systematic manner based on the evaluation of complex relative permittivity. In all cases conductivity can be calculated as a function of frequency and temperature from these evaluations. Previous information on electrical characteristics below 30 MHz in terms of permittivity and conductivity is retained in the Attachment to Annex 1 in view of its association with Recommendations ITU-R P.368 and ITU-R P.832. The new modelling method is fully compatible with this earlier information.

Keywords

Complex permittivity, conductivity, penetration depth, Earth's surface, water, vegetation, soil, ice

The ITU Radiocommunication Assembly,

considering

a) that the electrical characteristics may be expressed by three parameters: magnetic permeability, μ, electrical permittivity, ε, and electrical conductivity, σ;

b) that the permeability of the Earth's surface, μ, can normally be regarded as equal to the permeability in a vacuum;

c) that the electrical properties of the Earth's surface can be expressed by the complex permittivity or, equivalently, by the real part and imaginary part of the complex permittivity;

d) that information on the variation of the penetration depth with frequency is needed;

e) that knowledge of the electrical characteristics of the Earth's surface is needed for several purposes in propagation modelling, including ground-wave signal strength, ground reflection at a terrestrial terminal, interference between aeronautical and/or space borne stations due to reflections or scattering from the Earth's surface, and for Earth science applications;

f) that Recommendation ITU-R P.368 contains ground-wave propagation curves from 1 MHz to 30 MHz for different ground conditions characterised by permittivity and electrical conductivity;

g) that Recommendation ITU-R P.832 contains a world atlas of ground electrical conductivity for frequencies below 1 MHz,

recommends

that the information in Annex 1 should be used to model the electrical characteristics of the surface of the Earth.

Annex 1

1 Introduction

This Annex provides prediction methods that predict the electrical characteristics of the following Earth's surfaces for frequencies up to 1 000 GHz:

– Water
– Sea (i.e. Saline) Water
– Dry and Wet Ice
– Dry and Wet Soil (combination of sand, clay, and silt)
– Vegetation (above and below freezing)

2 Complex permittivity

The characteristics of the Earth's surface can be characterized by three parameters:

– the magnetic permeability, μ,
– the electrical permittivity, ε, and
– the electrical conductivity[1], σ.

Magnetic permeability is a measure of a material's ability to support the formation of a magnetic field within itself in response to an applied magnetic field; i.e. the magnetic flux density B divided by the magnetic field strength H. Electrical permittivity is a measure of a material's ability to oppose an electric field; i.e. the electrical flux density D divided by the electrical field strength E. Electrical conductivity is a measure of a material's ability to conduct an electric current; i.e. the ratio of the current density in the material to the electric field that causes the current flow.

Given an incident plane wave $\vec{E}(r,t) = \vec{E}_0 e^{j(\omega t - \boldsymbol{k} \cdot r)}$, with radial frequency ω, time t, magnetic permeability μ, electrical permittivity ε, and electrical conductivity σ, the propagation wave number vector $\vec{k}$, has a magnitude k given by

$$k = \sqrt{-j\omega\mu(\sigma + j\omega\varepsilon)} \tag{1a}$$

The vacuum values of permittivity, permeability, and conductivity are:

– Vacuum Permittivity $\varepsilon_0 = 8.854\,187\,817 \times 10^{-12}$ (F/m)
– Vacuum Permeability $\mu_0 = 4\pi \times 10^{-7}$ (N/A^2)
– Vacuum Conductivity $\sigma_0 = 0.0$ (S/m)

It is convenient to define the relative permittivity, ε_r, and the relative permeability, μ_r, relative to their vacuum values as follows:

– Relative Permittivity $\varepsilon_r = \frac{\varepsilon}{\varepsilon_0}$
– Relative Permeability $\mu_r = \frac{\mu}{\mu_0}$

where ε and μ are the associated permittivity and permeability of the medium. This Recommendation assumes $\mu = \mu_0$, in which case $\mu_r = 1$.

1 It is called electrical conductivity to differentiate it from other conductivities such as thermal conductivity and hydraulic conductivity. It is called hereinafter as conductivity.

As shown in equation (1a) the wavenumber depends on both σ and ε, not either separately. Also formulations of other physical parameters describing various radio wave propagation mechanisms such as scattering cross section, reflection coefficients, and refraction angles, depend on values of this combination. Furthermore, the square root of this combination is equivalent to the refractive index formulation used in characterizing the troposphere and the ionosphere. The refractive index is also used in characterizing different materials at the millimetre wave and optical frequency bands. Accordingly, to simplify the formulations describing various propagation mechanisms and to standardize terminologies of electrical characteristics at different frequency bands, the combination $\varepsilon - \frac{j\sigma}{\omega}$ is defined as the complex permittivity and used to describe the electrical characteristics of substances.

While permittivity refers to ε, relative permittivity refers to ε_r, and complex relative permittivity, defined as $\varepsilon_r' - j\,\varepsilon_r''$, refers to:

$$\varepsilon_r' - j\varepsilon_r'' = \frac{\varepsilon}{\varepsilon_0} - j\frac{\sigma}{\omega\varepsilon_0} \tag{1b}$$

where ε may be complex.

In equation (1b), ε_r' is the real part of the complex permittivity, and ε_r'' is the imaginary part of the complex permittivity. The real part of the complex relative permittivity, ε_r', is associated with the stored energy when the substance is exposed to an electromagnetic field. The imaginary part of the complex relative permittivity, ε_r'', influences energy absorption and is known as the loss factor. The minus sign in equation (1b) is associated with an electromagnetic field having time dependence of $e^{2j\pi ft}$ (f is frequency in Hz, and t is time in seconds). If the time dependence is $e^{-2j\pi ft}$, the minus (–) sign in equation (1b) is replaced by a plus (+) sign.

At frequencies up to 1 000 GHz, dissipation within the Earth's surface is attributed to either translational (conduction current) charge motion or vibrational (dipole vibration) charge motion, and the imaginary part of the complex relative permittivity, ε_r'' can be decomposed into two terms:

$$\varepsilon_r'' = \varepsilon_d'' + \frac{\sigma}{2\pi f\varepsilon_0} \tag{2}$$

where ε_d'' represents the dissipation due to displacement current associated with dipole vibration, and $\frac{\sigma}{2\pi f\varepsilon_0}$ represents the dissipation due to conduction current.

Conduction current consists of the bulk translation movement of free charges and is the only current at zero (i.e. dc) frequency. Conduction current is greater than displacement current at frequencies below the transition frequency, f_t, and the displacement current is greater than the conduction current at frequencies above the transition frequency, f_t. The transition frequency, f_t, defined as the frequency where the conduction and displacement currents are equal, is:

$$f_{\mathrm{t}} = \frac{\sigma}{2\pi\varepsilon_0\varepsilon_{\mathrm{d}}''} \tag{3}$$

For non-conducting (lossless) dielectric substances σ = 0, and hence $\varepsilon_r'' = \varepsilon_d''$. For some of those substances, such as dry soil and dry vegetation, $\varepsilon_d'' = 0$, and hence $\varepsilon_r'' = 0$ irrespective of the frequency, which is the case considered in § 2.1.2.3 of Recommendation ITU-R P.2040. On the other hand, for some other non-conducting substances, such as pure water and dry snow, ε_d'', and hence ε_r'', equal zero only at zero frequency. Accordingly, § 2.1.2.3 of Recommendation ITU-R P.2040 cannot be applied to those substances.

For conducting (lossy) dielectric substances, such as sea water and wet soil, the electrical conductivity σ has finite values different than zero. Accordingly, as the frequency tends to zero, the imaginary part of the complex relative permittivity of those substances tends to ∞ as it can be inferred from equation (3). In this case, it is easier to work with the conductivity σ instead of the imaginary part of the complex relative permittivity which can be written from equation (2) after setting $\varepsilon_d''= 0$ as follows:

$$\sigma = 2\pi\varepsilon_0 f\, \varepsilon_r'' = 0.05563 f_{\mathrm{GHz}} \varepsilon_r'' \tag{3a}$$

with f_{GHz} is the frequency in GHz. Generalizing the above formulation to other frequencies, as done by equation (12) of Recommendation ITU-R P.2040, yields the sum of two terms: one term gives the electrical conductivity and the other term accounts for the power dissipation associated with the displacement current.

This Recommendation provides prediction methods for the real and imaginary parts of the complex relative permittivity, ε_r' and ε_r''; and the accompanying example figures show trends of the real and imaginary parts of the complex relative permittivity with frequency under different environmental conditions.

2.1 Layered ground

The models in § 5 apply to homogeneous sub-surface soil; however, the sub-surface is rarely homogeneous. Rather, it consists of multiple layers of different thicknesses and different electrical characteristics that must be taken into account by introducing the concept of effective parameters to represent the homogeneous soil. Effective parameters can be used with the homogeneous smooth Earth ground-wave propagation curves of Recommendation ITU-R P.368.

3 Penetration depth

The extent to which the lower strata influence the effective electrical characteristics of the Earth's surface depends upon the penetration depth of the radio energy, δ, which is defined as the depth at which the amplitude of the field strength of electromagnetic radiation inside a material falls to 1/e (about 37%) of its original value at (or more properly, just beneath) the surface. The penetration depth, δ, in a homogeneous medium of complex relative permittivity ε_r ($\varepsilon_r = \varepsilon_r' - j\varepsilon_r''$) is given by:

$$\delta = \frac{\lambda}{2\pi}\sqrt{\frac{2}{\left[\sqrt{(\varepsilon_r')^2 + (\varepsilon_r'')^2} - \varepsilon_r'\right]}} \qquad \text{(m)} \tag{4}$$

where λ is the wavelength in metres. Note that as the imaginary part of the complex relative permittivity in equation (4) tends to zero, the penetration depth tends to infinity.

Figure 1 depicts typical values of penetration depth as a function of frequency for different types of Earth's surface components including pure water, sea water, dry soil, wet soil, and dry ice. The penetration depths for pure water and sea water are calculated at 20 °C, and the salinity of sea water is 35 g/kg. The penetration depths for dry soil and wet soil assume the volumetric water content is 0.07 and 0.5, respectively. Other soil parameters are the same as in Fig. 7. The penetration depth of dry ice is calculated at 0°C.

FIGURE 1

Penetration depth of surface types as a function of frequency

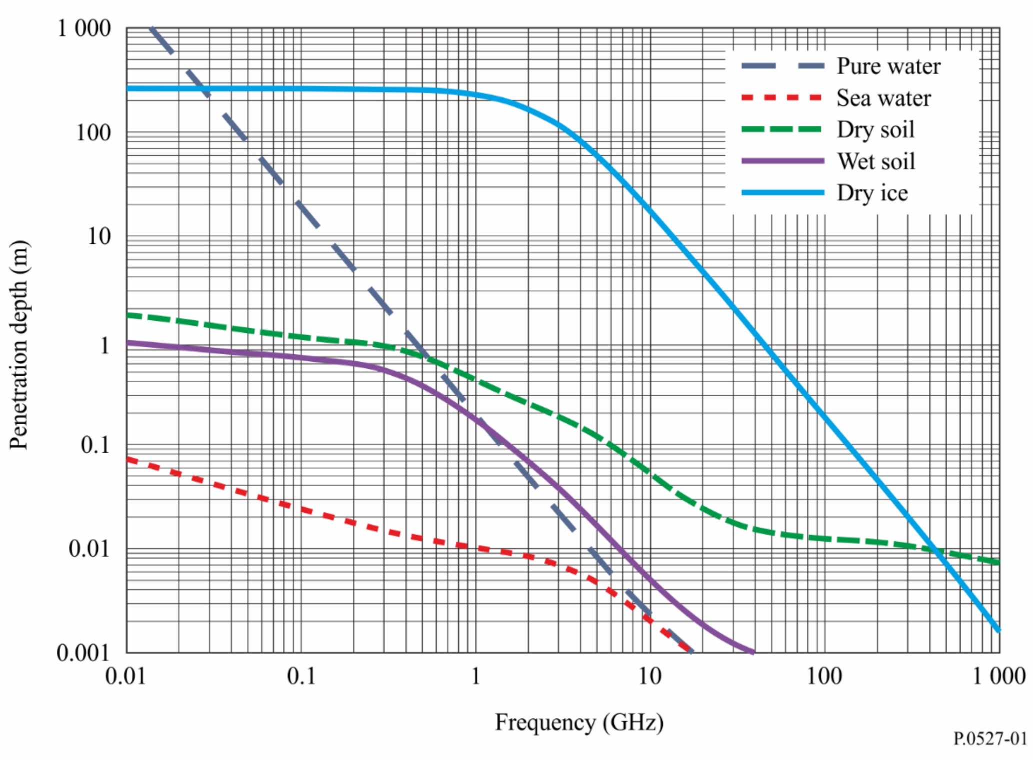

4 Factors determining the effective electrical characteristics of soil

The effective values of the electrical characteristics of the soil are determined by the nature of the soil, its moisture content, temperature, general geological structure, and the frequency of the incident electromagnetic radiation.

4.1 Nature of the soil

Although it has been established by numerous measurements that values of the electrical characteristics of soil vary with the nature of the soil, this variation may be due to its ability to absorb and retain moisture rather than the chemical composition of the soil. It has been shown that loam, which normally has a conductivity on the order of 10^{-2} S/m can, when dried, have a conductivity as low as 10^{-4} S/m, which is the same order as granite.

4.2 Moisture content

The moisture content of the ground is the major factor determining the permittivity and conductivity of the soil. Laboratory measurements have shown that as the moisture content of the ground increases from a low value, the permittivity and conductivity of the ground increase and reach their maximum values as the moisture content approaches the values normally found in such soils. At depths of one metre or more, the wetness of the soil at a particular site is typically constant. Although the wetness may increase during periods of rain, the wetness returns to its typical value after the rain has stopped due to drainage and surface evaporation.

The typical moisture content of a particular soil may vary considerably from one site to another due to differences in the general geological structure which provides different drainage.

4.3 Temperature

Laboratory measurements of the electrical characteristics of soil have shown that, at low frequencies conductivity increases by approximately 3% per degree Celsius, while permittivity is approximately constant over temperature. At the freezing point, there is generally a large decrease in both conductivity and permittivity.

4.4 Seasonal variation

The effects of seasonal variation on the electrical characteristics of the soil surface are due mainly to changes in water content and temperature of the top layer of the soil.

5 Complex relative permittivity prediction methods

The following sub-sections provide prediction methods to predict the complex relative permittivity of the following surfaces of the Earth:

– Pure water (§ 5.1.1)

– Sea (i.e. saline) water (§ 5.1.2)

– Pure ice (§ 5.1.3.1)

– Sea ice brine (§ 5.1.3.2)

– Sea ice (first year ice and multi-year ice) (§ 5.1.3.3)

– Snow (dry snow and wet snow) (§ 5.1.4)

– Sea foam (§ 5.1.5)

– Soil (combination of sand, clay, silt, and water) (§ 5.2)

– Vegetation (above and below freezing) (§ 5.3).

In this section, the subscripts of the real and imaginary parts of the complex relative permittivity are: "*pw*" for pure water, "*sw*" for sea water, "*ice*" for pure ice, "*b*" for sea ice brine, "*m*" for sea ice, "*ds*" for dry snow, "*ws*" for wet snow, "*f*" for sea foam, and "*soil*" for soil. The complex relative permittivity of pure water, sea water, pure ice, and sea ice brine are based on the characteristics of their individual constituents, and, consequently, the complex relative permittivity of sea ice, snow, sea foam, soil, and vegetation are based on the mixing of two or more constituents.

5.1 Water

This sub-section provides prediction methods for the complex relative permittivity of pure water, sea water, sea foam, ice (pure ice, sea ice brine, and sea ice), and snow (dry snow and wet snow).

Sections 5.1.1 and 5.1.2 are valid for temperatures of -4 ºC $\leq T \leq$ 40 ºC and salinities of 0 ppt $\leq S \leq$ 40 ppt where ppt is parts per thousand.

5.1.1 Pure water

The complex relative permittivity of pure water, ε_{pw}, is a function of frequency, f_{GHz} (GHz), and temperature, T (ºC):

$$\varepsilon_{pw} = \varepsilon'_{pw} - j\,\varepsilon''_{pw} \tag{5}$$

$$\varepsilon'_{pw} = \frac{\varepsilon_s - \varepsilon_1}{1+(f_{\mathrm{GHz}}/f_1)^2} + \frac{\varepsilon_1 - \varepsilon_\infty}{1+(f_{\mathrm{GHz}}/f_2)^2} + \varepsilon_\infty \tag{6}$$

$$\varepsilon''_{pw} = \frac{(f_{\mathrm{GHz}}/f_1)(\varepsilon_s - \varepsilon_1)}{1+(f_{\mathrm{GHz}}/f_1)^2} + \frac{(f_{\mathrm{GHz}}/f_2)(\varepsilon_1 - \varepsilon_\infty)}{1+(f_{\mathrm{GHz}}/f_2)^2} \tag{7}$$

where:

$$\varepsilon_s = 77.66 + 103.3\,\Theta \tag{8}$$

$$\varepsilon_1 = 0.0671\varepsilon_s \tag{9}$$

$$\varepsilon_\infty = 3.52 - 7.52\,\Theta \tag{10}$$

$$\Theta = \frac{300}{T+273.15} - 1 \tag{11}$$

and f_1 and f_2 are the Debye relaxation frequencies:

$$f_1 = 20.20 - 146.4\ \Theta + 316\,\Theta^2 \qquad \text{(GHz)} \tag{12}$$

$$f_2 = 39.8\,f_1 \qquad \text{(GHz)} \tag{13}$$

5.1.2 Sea water

The complex relative permittivity of sea (saline) water, ε_{sw}, is a function of frequency, f_{GHz} (GHz), temperature, T (°C), and salinity S (g/kg or ppt)[2].

$$\varepsilon_{sw} = \varepsilon'_{sw} - j\,\varepsilon''_{sw} \tag{14}$$

$$\varepsilon'_{sw} = \frac{\varepsilon_{ss}-\varepsilon_{1s}}{1+(f_{\mathrm{GHz}}/f_{1s})^2} + \frac{\varepsilon_{1s}-\varepsilon_{\infty s}}{1+(f_{\mathrm{GHz}}/f_{2s})^2} + \varepsilon_{\infty s} \tag{15}$$

$$\varepsilon''_{sw} = \frac{(f_{\mathrm{GHz}}/f_{1s})(\varepsilon_{ss}-\varepsilon_{1s})}{1+(f_{\mathrm{GHz}}/f_{1s})^2} + \frac{(f_{\mathrm{GHz}}/f_{2s})(\varepsilon_{1s}-\varepsilon_{\infty s})}{1+(f_{\mathrm{GHz}}/f_{2s})^2} + \frac{18\,\sigma_{sw}}{f_{\mathrm{GHz}}} \tag{16}$$

where:

$$\varepsilon_{ss} = \varepsilon_s \exp(-3.33330\times10^{-3}S + 4.74868\times10^{-6}S^2) \tag{17}$$

$$f_{1s} = f_1\left(1 + S\begin{pmatrix}2.3232\times10^{-3} - 7.9208\times10^{-5}T + 3.6764\times10^{-6}T^2\\ + 3.5594\times10^{-7}T^3 + 8.9795\times10^{-9}T^4\end{pmatrix}\right) \quad \text{(GHz)} \tag{18}$$

$$\varepsilon_{1s} = \varepsilon_1 \exp(-6.28908\times10^{-3}S + 1.76032\times10^{-4}S^2 - 9.22144\times10^{-5}TS) \tag{19}$$

$$f_{2s} = f_2\left(1 + S(-1.99723\times10^{-2} + 1.81176\times10^{-4}T)\right) \qquad \text{(GHz)} \tag{20}$$

$$\varepsilon_{\infty s} = \varepsilon_\infty\left(1 + S(-2.04265\times10^{-3} + 1.57883\times10^{-4}T)\right) \tag{21}$$

Values of ε_s, ε_1, ε_∞, $f_1$and f_2 are obtained from equations (8), (9), (10), (12) and (13). Furthermore, σ_{sw} is given by

$$\sigma_{sw} = \sigma_{35}\,R_{15}R_{T15} \quad \text{(S/m)} \tag{22}$$

$$\sigma_{35} = 2.903602 + 8.607\times10^{-2}\,T + 4.738817\times10^{-4}\,T^2$$
$$-2.991\times10^{-6}\,T^3 + 4.3047\times10^{-9}\,T^4 \tag{23}$$

$$R_{15} = S\,\frac{(37.5109+5.45216S+1.4409\times10^{-2}\,S^2)}{(1004.75+182.283\,S+S^2)} \tag{24}$$

$$R_{T15} = 1 + \frac{\alpha_0(T-15)}{(\alpha_1+T)} \tag{25}$$

$$\alpha_0 = \frac{(6.9431+3.2841S-9.9486\times10^{-2}S^2)}{(84.850+69.024\,S+S^2)} \tag{26}$$

$$\alpha_1 = 49.843 - 0.2276\,S + 0.198\times10^{-2}\,S^2 \tag{27}$$

---

[2] The term “ppt” stands for “parts per thousand”.

The complex relative permittivity of pure water given in equations (5) to (7) is a special case of equation (14) to (16) where $S = 0$. The complex relative permittivity of pure water ($S = 0$ g/kg) and sea water ($S = 35$ g/kg) vs. frequency are shown in Fig. 2 for $T = 20$ °C and in Fig. 3 for $\mathrm{T} = 0$ °C.

FIGURE 2

Complex relative permittivity of pure and sea water as a function of frequency
($T = 20$ °C)

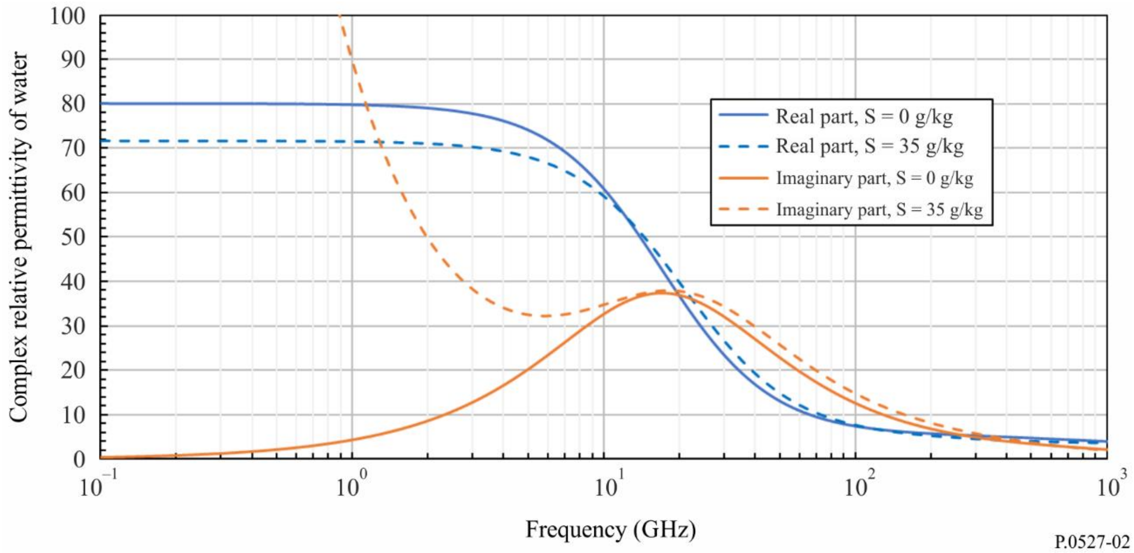

FIGURE 3

Complex relative permittivity of pure and sea water as a function of frequency
($T = 0$ °C)

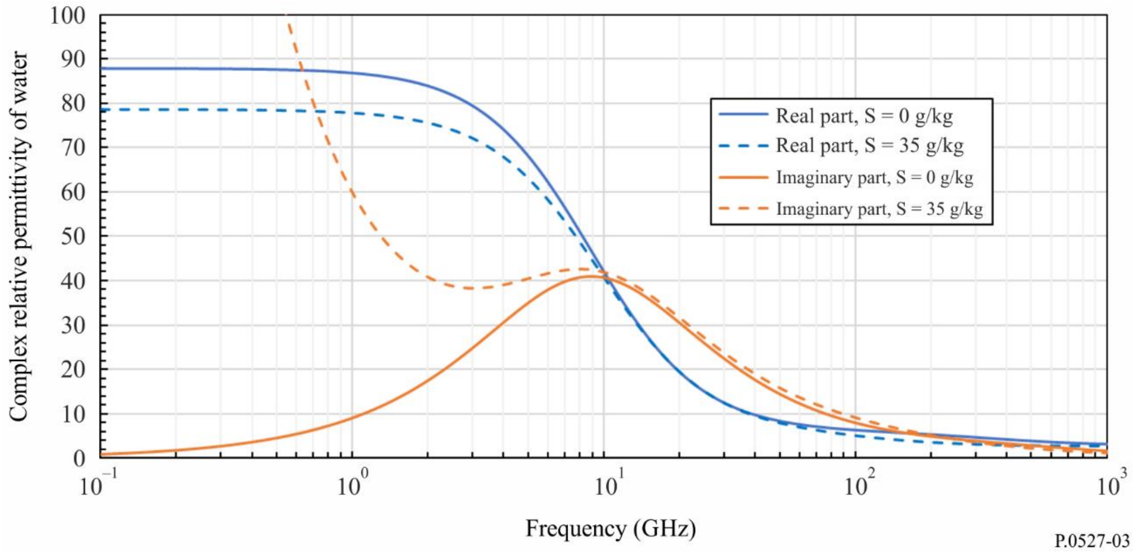

5.1.3 Ice

This section provides prediction methods for the complex relative permittivity of pure ice, sea ice brine and sea ice.

5.1.3.1 Pure ice

Pure ice is composed of frozen pure water (i.e. -60 ºC $\leq T_{ice} \leq 0$ ºC). The complex relative permittivity of pure ice, ε_{ice}, is given by:

$$\varepsilon_{ice} = \varepsilon'_{ice} - j\,\varepsilon''_{ice} \tag{28}$$

The real part of the complex relative permittivity of pure ice, ε'_{ice}, is a function of temperature, T_{ice} (°C), and is independent of frequency:

$$\varepsilon'_{ice} = 3.1884 + 0.00091\,T_{ice} \tag{29}$$

and the imaginary part of the complex relative permittivity of pure ice, ε''_{ice}, is a function of temperature T_{ice} (°C), for frequencies, f_{GHz} (GHz), up to 1 000 GHz:

$$\varepsilon''_{ice} = \frac{A}{f_{\mathrm{GHz}}} + B f_{\mathrm{GHz}} \tag{30}$$

where

$$A = (0.00504 + 0.0062\Theta)\exp(-22.1\Theta) \tag{31}$$

$$B = \frac{0.0207}{T_{ice}+273.15}\,\frac{\exp(-\tau)}{(\exp(-\tau)-1)^2} + 1.16\times10^{-11} f_{GHz}^2 + \exp(-9.963 + 0.0372 T_{ice}) \tag{32}$$

$$\tau = \frac{335}{T_{ice}+273.15} \tag{33}$$

and

$$\theta = \frac{300}{T_{ice}+273.15} - 1 \tag{34}$$

The real (ε'_{ice}) and imaginary (ε''_{ice}) parts of the complex relative permittivity of pure ice vs frequency for $T_{ice} = 0$ °C are shown in Fig. 4.

FIGURE 4

Complex relative permittivity of pure ice vs frequency ($T_{ice} = 0$ °C)

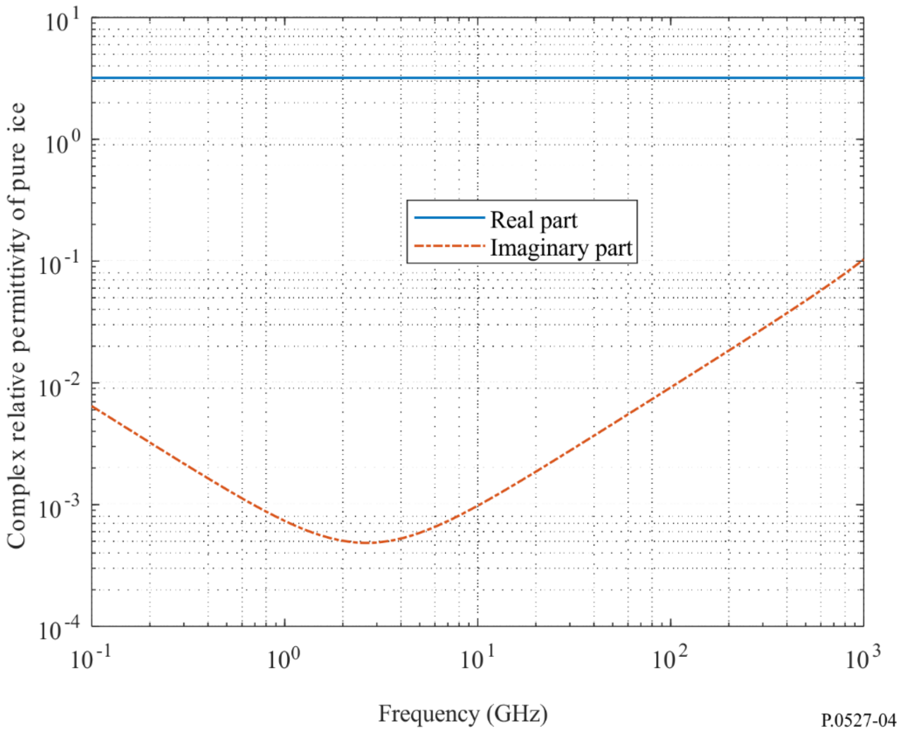

5.1.3.2 Sea ice brine

Sea ice brine is pure water with dissolved salt droplets that exists during the formation of sea ice. The complex relative permittivity of sea ice brine, ε_b, is:

$$\varepsilon_b = \varepsilon_b' - j\varepsilon_b'' \tag{35}$$

For temperatures −30 ºC ≤ T_{ice} ≤ −2 ºC and frequencies, f_{GHz} (GHz), up to 1 000 GHz, ε_b' and ε_b'' are:

$$\varepsilon_b' = \varepsilon_{b\infty} + \frac{\varepsilon_{bs} - \varepsilon_{b\infty}}{1+(2\pi\tau f_{GHz})^2} \tag{36}$$

$$\varepsilon_b'' = \frac{2\pi\tau f_{GHz}(\varepsilon_{bs}-\varepsilon_{b\infty})}{1+(2\pi\tau f_{GHz})^2} + \frac{18\,\sigma_b}{f_{GHz}} \tag{37}$$

where:

$$\varepsilon_{b\infty} = \frac{82.79 + 8.19\,T_{ice}^2}{15.68 + T_{ice}^2} \tag{38a}$$

$$\varepsilon_{bs} = \frac{939.66 - 19.068\,T_{ice}}{10.737 - T_{ice}} \tag{38b}$$

$$2\pi\tau = 0.10990 + 0.13603 \times 10^{-2} T_{ice} + 0.20894 \times 10^{-3} T_{ice}^2 + 0.28167 \times 10^{-5} T_{ice}^3 \tag{38c}$$

T_{ice} (°C) is the temperature, and σ_b (S/m) is the conductivity given by:

$$\sigma_b = \begin{cases} -T_{ice}\exp(0.5193 + 0.08755\,T_{ice}), & T_{ice} \geq -22.9\,°C \\ -T_{ice}\exp(1.0334 + 0.1100\,T_{ice}), & T_{ice} < -22.9\,°C \end{cases} \tag{39}$$

The real (ε_b') and imaginary (ε_b'') parts of the complex relative permittivity of sea ice brine vs frequency for T_{ice} = −5 °C and −25 °C are shown in Figs 5 and 6, respectively.

FIGURE 5

Complex relative permittivity of sea ice brine vs frequency (T_{ice} = −5°C)

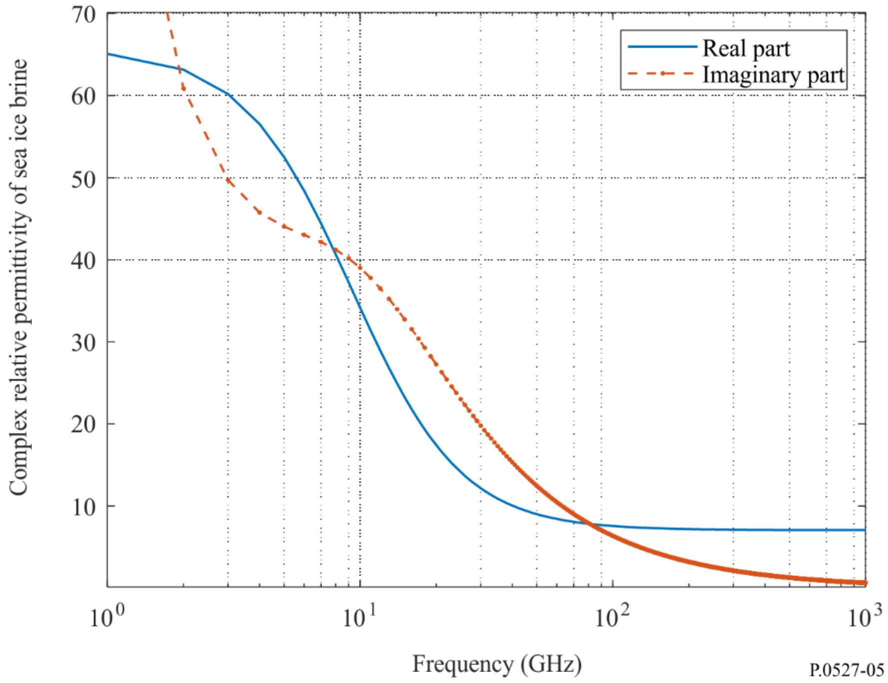

FIGURE 6

Complex relative permittivity of sea ice brine vs frequency (T_{ice} = −25 °C)

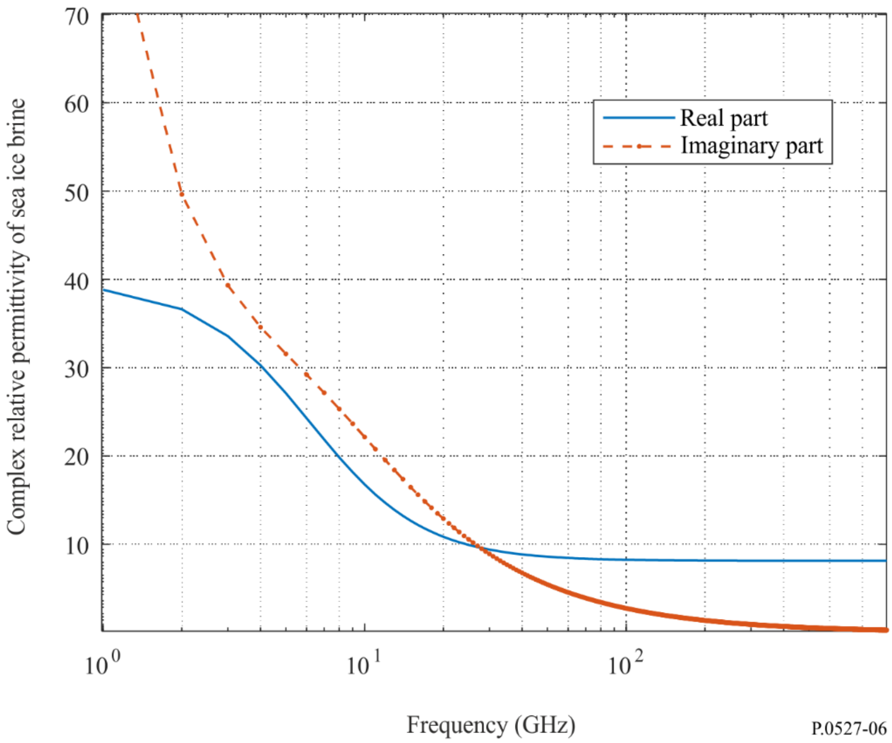

5.1.3.3 Sea ice

There are two types of sea ice: a) first-year ice and b) multi-year ice.

First-year ice is composed of pure ice and brine pockets, where the shape of the brine pockets depends on whether the first-year ice is frazil ice or columnar ice. Frazil ice is a collection of loose, randomly oriented needle-shaped ice crystals, and columnar ice is a collection of vertically oriented needle-shaped ice crystals. First-year ice has a maximum thickness between 0.3 m and 2 m.

Multi-year ice is ice that has survived at least one melt season and contains much less brine and more air pockets than first-year ice. Multi-year ice is typically 2 to 4 m thick, and the air pockets are spherically shaped.

For first-year ice, the brine volume fraction, v_b, is given by:

$$v_b = \frac{\rho_{ice}\, S_{ice}}{F_1(T_{ice}) - \rho_{ice}\, S_{ice} F_2(T_{ice})} \tag{40}$$

where ρ_{ice} (g/cm^3) is the sea ice density given by:

$$\rho_{ice} = 0.917 - 1.403 \times 10^{-4}\, T_{ice} \tag{41}$$

T_{ice} (°C) is the ice temperature, −30 °C ≤ T_{ice} ≤ −2 °C and S_{ice} (ppt) is the sea ice salinity, where:

$$S_{ice} = \begin{cases} 7.88 - 1.59\, h_{ice}, & h_{ice} > 0.3573\, m \\ 14.24 - 19.39\, h_{ice}, & h_{ice} \le 0.3573\, m \end{cases} \tag{42}$$

and h_{ice} (m) is the sea ice thickness. F_1 and F_2 are calculated as follows using the coefficients in Table 1:

$$F_i(T_{ice}) = \alpha_0 + \alpha_1 T_{ice} + \alpha_2 T_{ice}^2 + \alpha_3 T_{ice}^3,\ i = 1, 2 \tag{43}$$

TABLE 1

Coefficients α_0, α_1, α_2, and α_3

Coefficient	$-30°C \le T_{ice} \le -22.9°C$		$-22.9°C \le T_{ice} \le -2°C$	
	$F_1(T_{ice})$	$F_2(T_{ice})$	$F_1(T_{ice})$	$F_2(T_{ice})$
α_0	9 899	8.547	−4.732	0.089 03
α_1	1 309	1.089	−22.45	−0.017 63
α_2	55.27	0.045 18	−0.639 7	−0.000 533
α_3	0.716	0.000 581 9	−0.010 74	−0.000 008 801

5.1.3.3.1 Complex relative permittivity of first-year ice

This sub-section provides prediction methods for predicting the complex relative permittivity of frazil and columnar first-year ice.

The complex relative permittivity prediction methods in this section are applicable at temperatures of $-30°C \le T_{ice} \le -2°C$ and frequencies up to 100 GHz.

a) Complex relative permittivity of frazil sea ice

For frazil ice, where the brine pockets are randomly oriented needles, the complex relative permittivity is isotropic and is given by:

$$\varepsilon_m = \frac{-B + \sqrt{B^2 - 4AC}}{2A} \tag{44}$$

where:

$$A = 3 \tag{45a}$$

$$B = (3 - 5v_b)(\varepsilon_b - \varepsilon_{ice}) \tag{45b}$$

$$C = -(3 - v_b)\varepsilon_b\varepsilon_{ice} - v_b\,(\varepsilon_b)^2 \tag{45c}$$

ε_{ice}, ε_b, and v_b are calculated from equations (28), (35) and (40), respectively.

The real ($Re\{\varepsilon_m\}$) and imaginary ($Im\{\varepsilon_m\}$) parts of the complex relative permittivity of first-year frazil sea ice vs frequency for T_{ice} −5°C are shown in Fig. 7.

FIGURE 7

Complex relative permittivity of first year frazil sea ice vs frequency (T_{ice}= −5°C and h_{ice} = 0.2 m)

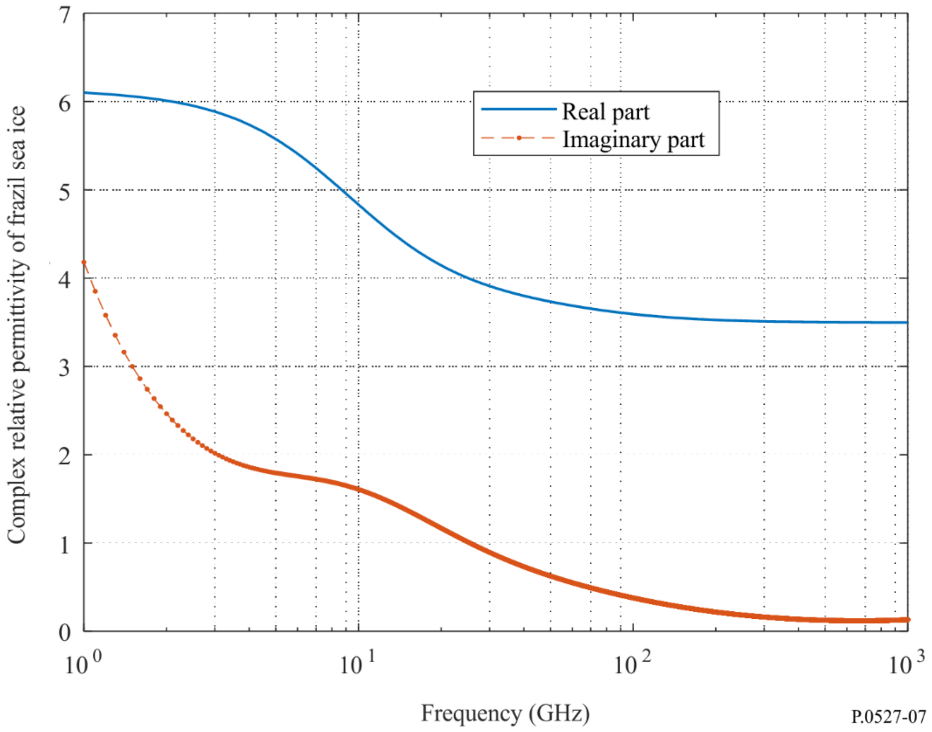

b) Complex relative permittivity of columnar ice

For columnar ice, where the brine pockets are vertically oriented needles, the complex relative permittivity is anisotropic. The components ε_{mx}, ε_{my}, and ε_{mz}, where the x and y axes are parallel to the surface of the Earth, and the z axis is normal to the surface of the Earth, are given by:

$$\varepsilon_{mx} = \varepsilon_{my} = \frac{-B+\sqrt{B^2-4AC}}{2A} \tag{46}$$

$$\varepsilon_{mz} = \varepsilon_{ice} + v_b\,(\varepsilon_b - \varepsilon_{ice}) \tag{47}$$

where:

$$A = 1 \tag{48a}$$

$$B = (1-2v_b)(\varepsilon_b - \varepsilon_{ice}) \tag{48b}$$

$$C = -\varepsilon_b\varepsilon_{ice} \tag{48c}$$

ε_{ice}, ε_b, and v_b are calculated from equations (28), (35), and (40) respectively.

The real ($Re\{\varepsilon_{mx,y}\}$) and imaginary ($Im\{\varepsilon_{mx,y}\}$) parts of the complex relative permittivity of columnar sea ice vs frequency for T_{ice} = −5°C in the horizontal (i.e. x and y) directions are shown in Fig. 8, and the real ($Re\{\varepsilon_{mz}\}$) and imaginary ($Im\{\varepsilon_{mz}\}$) parts of the complex relative permittivity of columnar sea ice vs frequency for T_{ice} = −5°C in the vertical (i.e. z) direction are shown in Fig. 9.

FIGURE 8

Complex relative permittivity of first-year columnar sea ice in the horizontal (x and y) direction vs frequency (T_{ice} = −5°C and $h_{ice} = 0.2$ m)

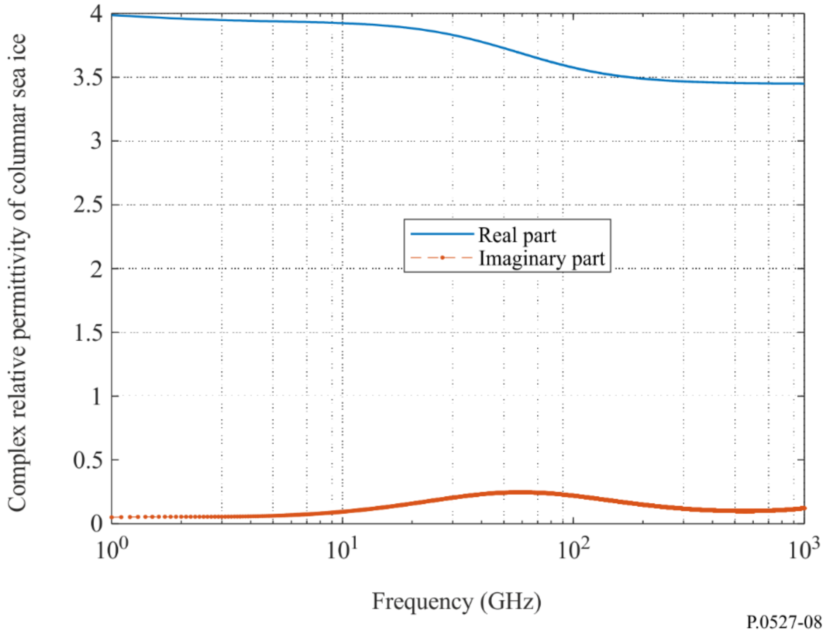

FIGURE 9

Complex relative permittivity of first-year columnar sea ice in the vertical (z) direction vs frequency (T_{ice} = −5°C and $h_{ice} = 0.2$ m)

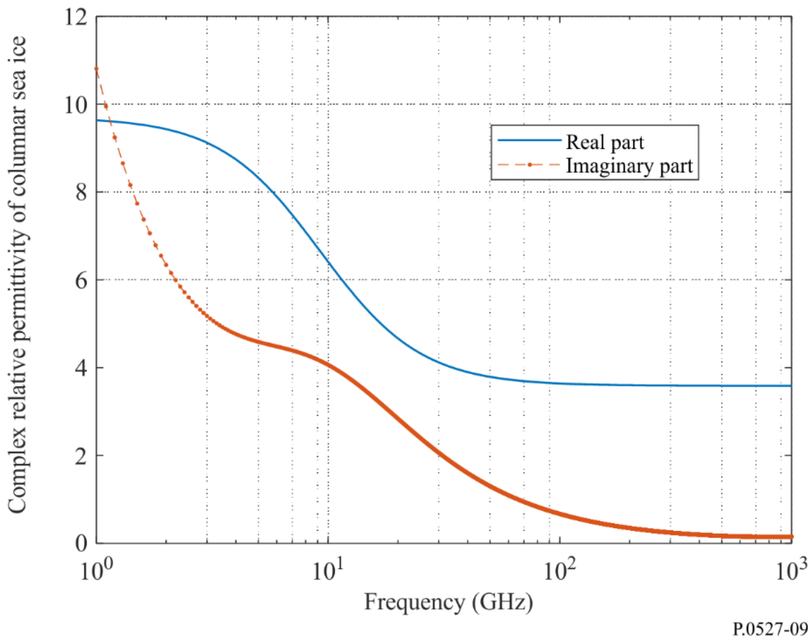

5.1.3.3.2 Complex relative permittivity of multi-year ice

For multi-year ice, which is a mixture of pure ice and spherical air pockets, the complex relative permittivity, ε_m, is isotropic and is given by:

$$\varepsilon_m = \frac{-B - \sqrt{B^2 - 4AC}}{2A} \tag{49}$$

where:

$$A = 2 \tag{50a}$$

$$B = 1 - 2\varepsilon_{ice} - 3v_a(1 - \varepsilon_{ice}) \tag{50b}$$

$$C = -\varepsilon_{ice} \tag{50c}$$

ε_{ice} is the complex relative permittivity of pure ice given by equation (28), and v_a is the air volume fraction.

The above complex relative permittivity prediction method is applicable at temperatures of $-30°C \leq T \leq -2°C$ and frequencies up to 100 GHz.

5.1.4 Snow

The complex relative permittivity prediction methods in this section are applicable at temperatures of $-60°C \leq T \leq 0°C$ and frequencies up to 100 GHz.

5.1.4.1 Dry snow

The complex relative permittivity of dry snow, ε_{ds}, is:

$$\varepsilon_{ds} = \varepsilon'_{ds} - j\varepsilon''_{ds} \tag{51}$$

where:

$$\varepsilon'_{ds} = \begin{cases} 1 + 1.9\rho_{ds}, & \rho_{ds} \leq 0.5\ g/cm^3 \\ 0.51 + 2.88\rho_{ds}, & \rho_{ds} \geq 0.5\ g/cm^3 \end{cases} \tag{52}$$

$$\varepsilon''_{ds} = 3\varepsilon''_{ice}\, f_{ice}\, \frac{(\varepsilon'_{ds})^2(2\varepsilon'_{ds}+1)}{(\varepsilon'_{ice}+2\varepsilon'_{ds})\left[\varepsilon'_{ice} + 2(\varepsilon'_{ds})^2\right]} \tag{53}$$

ρ_{ds} is the dry snow density in $\mathrm{g/cm^3}$, and $f_{ice} = \rho_{ds}/\rho_{ice}$, where $\rho_{ice} = 0.916\ \mathrm{g/cm^3}$.

The real (ε'_{ds}) and imaginary (ε''_{ds}) parts of the complex relative permittivity of dry snow vs frequency for $\rho_{ds} = 0.4\ \mathrm{g/cm^3}$, $\rho_{ice} = 0.916\ \mathrm{g/cm^3}$, and $T_{ice} = -10°C$ are shown in Fig. 10.

FIGURE 10

The complex relative permittivity of dry snow vs frequency
($\rho_{ds} = 0.4\ g/cm^3$, $\rho_{ice} = 0.916\ g/cm^3$, and $T_{ice} = -10$°C)

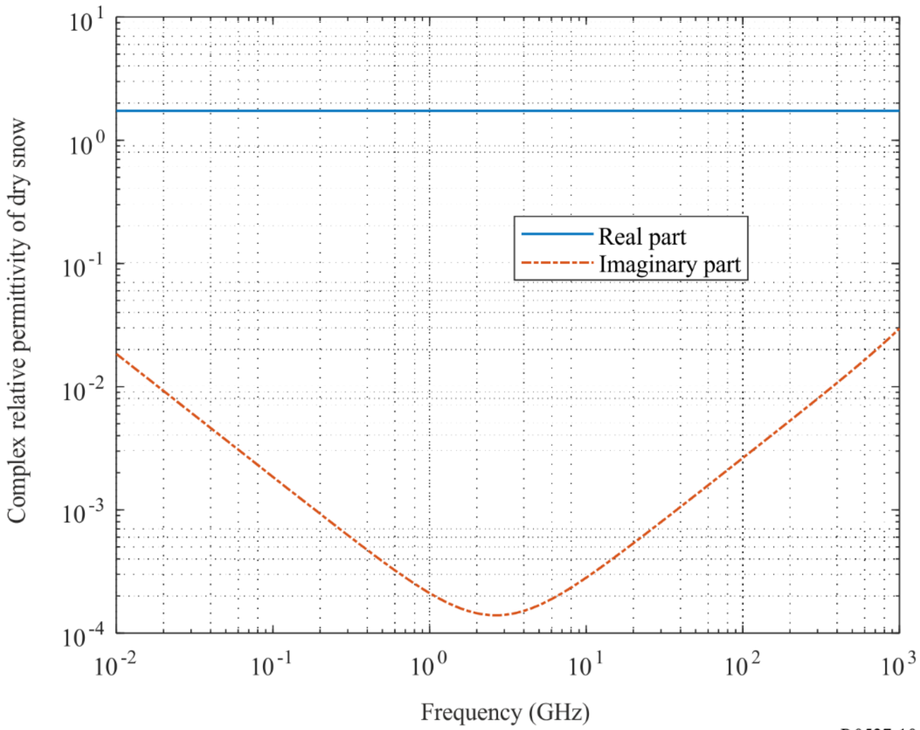

P.0527-10

5.1.4.2 Wet snow

Wet snow is a mixture of dry snow and pure water. The complex relative permittivity of wet snow, ε_{ws}, is:

$$\varepsilon_{ws} = \frac{-B + \sqrt{B^2 - 4AC}}{2A} \tag{54}$$

where:

$$A = 2 \tag{55a}$$

$$B = \varepsilon_{pw} - 2\varepsilon_{ds} - 3F_{wc}\left(\varepsilon_{pw} - \varepsilon_{ds}\right) \tag{55b}$$

$$C = -\,\varepsilon_{pw}\varepsilon_{ds} \tag{55c}$$

F_{wc} $(0 \le F_{wc} \le 1)$ is the liquid water volume fraction (m^3/m^3); and ε_{pw} and ε_{ice} are the complex relative permittivities of pure water and dry snow from equations (5) and (51), respectively. The real $(Re\{\varepsilon_{ws}\})$ and imaginary $(Im\{\varepsilon_{ws}\})$ parts of the complex relative permittivity of wet snow vs liquid water volume fraction for $f_{\text{GHz}} = 60$ GHz and $T = 0$°C are shown in Fig. 11.

FIGURE 11

Complex relative permittivity of wet snow vs liquid water content volume fraction (f_{GHz} = 60 GHz and T = 0°C)

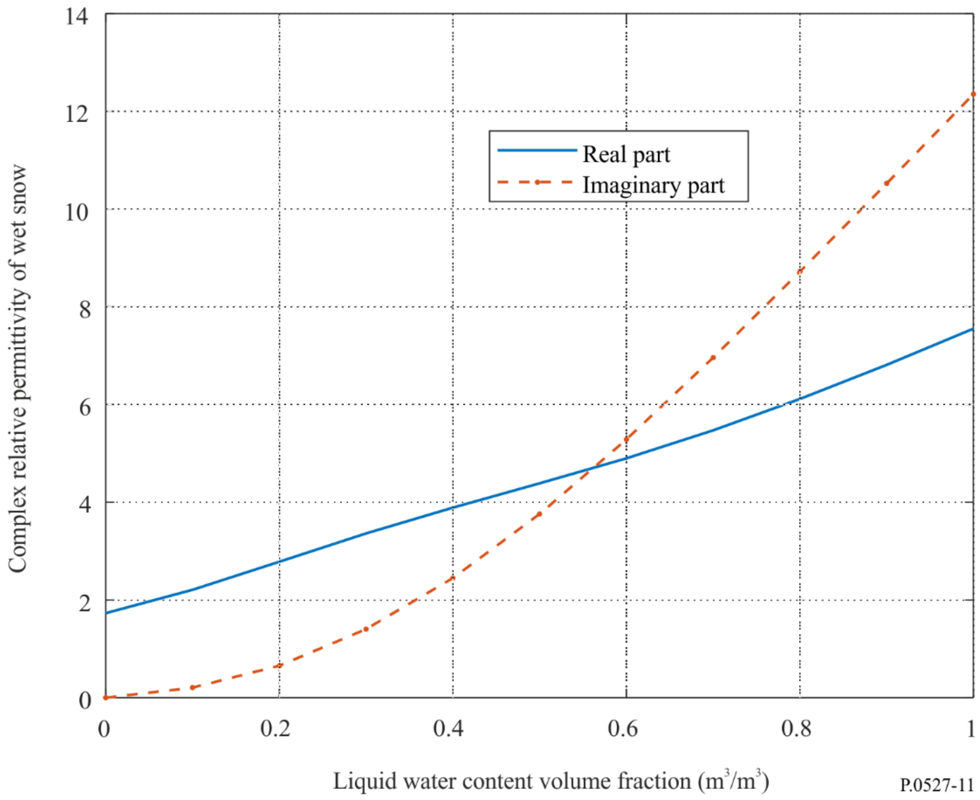

P.0527-11

5.1.5 Sea foam

Sea foam, created by the agitation of sea water by breaking waves adjacent to the shore, is composed of sea water and trapped air bubbles. The complex relative permittivity of sea foam, ε_f, is:

$$\varepsilon_f = \left(f_a + (1 - f_a)\sqrt{\varepsilon_{sw}}\right)^2 \tag{56}$$

where f_a $(0 \leq f_a \leq 1)$ is the void volume fraction, and ε_{sw} is the complex relative permittivity of sea water from equation (14). The void volume fraction (m^3/m^3), the ratio of the volume of air bubbles to the total volume, has its maximum value at the air-foam interface and its minimum value at the foam-sea water interface. The complex relative permittivity prediction method in (56) is applicable at temperatures of $-4°C \leq T \leq 40°C$ and frequencies up to 100 GHz.

The real ($Re\{\varepsilon_f\}$) and imaginary ($Im\{\varepsilon_f\}$) parts of the complex relative permittivity of sea foam vs void volume fraction for $f_{\text{GHz}} = 60$ GHz, $S = 35$ ppt, and $T = 20$°C are shown in Fig. 12.

FIGURE 12

Complex relative permittivity of sea foam vs void volume fraction
(f_{GHz} = 60 GHz, T = 20°C, and S = 35 ppt)

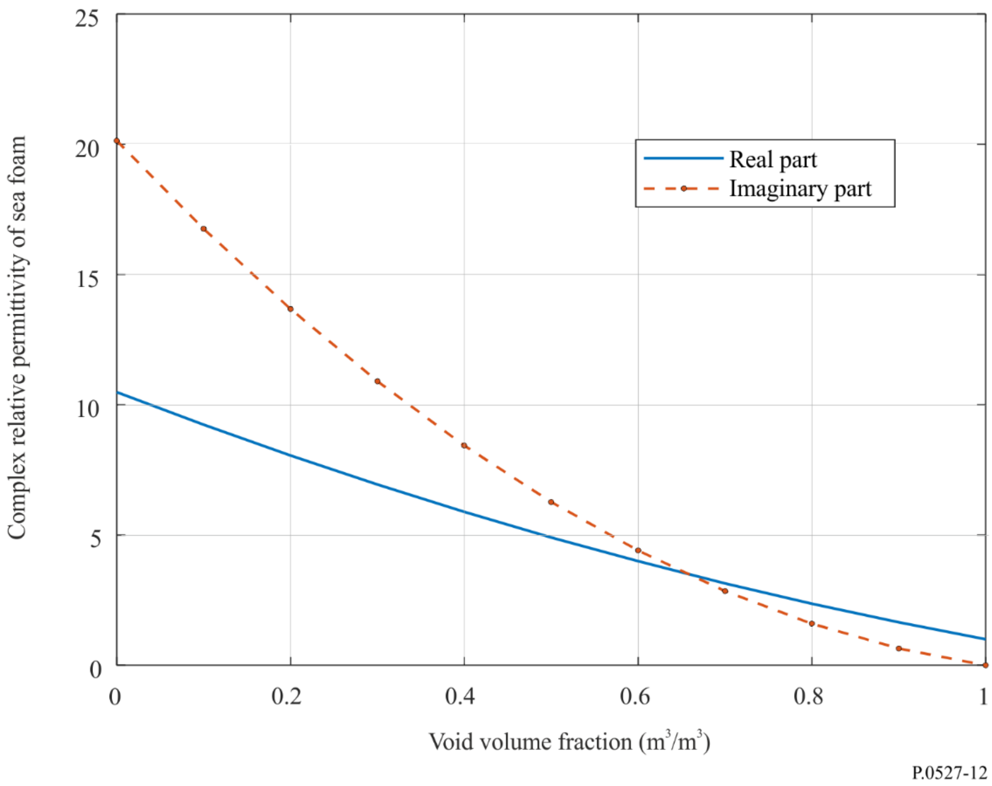

5.2 Soil

The complex relative permittivity of soil, ε_{soil}, is a function of frequency, f_{GHz} (GHz), temperature, T (°C), soil composition, and volumetric water content.

The soil composition is characterized by the percentages by volume of the following dry soil constituents which are available from field surveys and laboratory analysis: a) P_{sand} = % sand; b) P_{clay} = % clay; and c) P_{silt} = % silt.

The soil composition is also characterized by: a) the specific gravity (i.e. the mass density of soil divided by the mass density of water) of the dry mixture of soil constituents, ρ_s (g/cm^3); b) the volumetric water content, m_v (i.e. the water volume divided by total soil volume for a given soil sample, (m^3/m^3)); and c) the bulk density, ρ_b (g/cm^3) (i.e. the mass of soil in a given volume of soil). While the bulk density of the soil, ρ_b, is not easily measured directly, it can be derived from the percentages of the dry constituents. If a local pseudo-transfer function is not available, the following empirical pseudo-transfer function can be used:

$$\rho_b = 1.07256 + 0.078886 ln(P_{sand}) + 0.038753 ln\left(P_{clay}\right) + 0.032732\, ln(P_{silt}) \quad (57)$$

If the percentage of any constituent is less than 1%, the corresponding term in equation (57) should be omitted. The constituent percentages of the included terms should sum to 100%.

The soil temperature and volumetric water content can be obtained from global maps provided by space-borne remote sensing systems, and the soil texture can be obtained from geologic data bases such as HWSD1.21 (Harmonized World Soil Databases Version 1.21) and GLDAS (Global Land Data Assimilation System). In absence of local data, Table 2 can be used.

Table 2 shows typical constituent percentages, specific gravities, and bulk densities for four representative soil types.

TABLE 2

Physical parameters of various soil types

Soil designation textural class	1 Sandy loam	2 Loam	3 Silty loam	4 Silty clay
% Sand	51.52	41.96	30.63	5.02
% Clay	13.42	8.53	13.48	47.38
% Silt	35.06	49.51	55.89	47.60
ρ_s	2.66	2.70	2.59	2.56
ρ_b (g cm^{-3})	1.6006	1.5781	1.5750	1.4758

FIGURE 13

Soil texture triangle

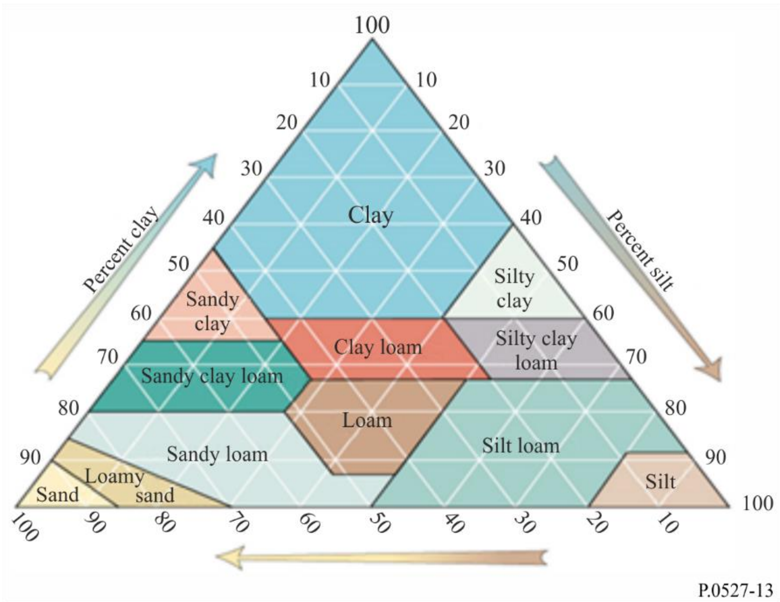

The soil designation textural class reported in the first row of Table 1 is based on the soil texture triangle depicted in Fig. 13.

This prediction method considers soil as a mixture of four components: a) soil particles composed of a combination of clay, sand, and silt, b) air, c) bound water (water attached to soil particles by forces such as surface tension, where the thickness of the water layer and its dielectric constant and relaxation frequencies are unknown), and d) free water (also known as bulk water that flows freely within soil bores). The complex relative permittivity of soil, ε_{soil}, of this four component mixture is

$$\varepsilon_{soil} = \varepsilon'_{soil} - j\varepsilon''_{soil} \tag{58}$$

where:

$$\varepsilon'_{soil} = \left[1 + \frac{\rho_b}{\rho_s}\left(\{\varepsilon'_{sm}\}^{\alpha} - 1\right) + m_{\mathrm{v}}^{\beta'}\left(\varepsilon'_{fw}\right)^{\alpha} - m_{\mathrm{v}}\right]^{1/\alpha} \tag{59}$$

$$\varepsilon''_{soil} = \left[m_{\mathrm{v}}^{\beta''}\left(\varepsilon''_{fw}\right)^{\alpha}\right]^{1/\alpha} \tag{60}$$

$$\varepsilon'_{sm} = (1.01 + 0.44\,\rho_s)^2 - 0.062 \tag{61}$$

$$\beta' = 1.2748 - 0.00519\,P_{sand} - 0.00152\,P_{clay} \tag{62}$$

$$\beta'' = 1.33797 - 0.00603\,P_{sand} - 0.00166\,P_{clay} \tag{63}$$

and

$$\alpha = 0.65 \tag{64}$$

ε'_{fw} and ε''_{fw} are the real and the imaginary parts of the complex relative permittivity of free water:

$$\varepsilon'_{fw} = \frac{\varepsilon_s - \varepsilon_1}{1+(f_{\mathrm{GHz}}/f_1)^2} + \frac{\varepsilon_1 - \varepsilon_\infty}{1+(f_{\mathrm{GHz}}/f_2)^2} + \varepsilon_\infty + \frac{18\,\sigma'_{eff}}{f_{\mathrm{GHz}}}\frac{(\rho_s - \rho_b)}{\rho_s m_{\mathrm{v}}} \tag{65}$$

$$\varepsilon''_{fw} = \frac{(f_{\mathrm{GHz}}/f_1)(\varepsilon_s - \varepsilon_1)}{1+(f_{\mathrm{GHz}}/f_1)^2} + \frac{(f_{\mathrm{GHz}}/f_2)(\varepsilon_1 - \varepsilon_\infty)}{1+(f_{\mathrm{GHz}}/f_2)^2} + \frac{18\,\sigma''_{eff}}{f_{\mathrm{GHz}}}\frac{(\rho_s - \rho_b)}{\rho_s m_{\mathrm{v}}} \tag{66}$$

where ε_s, ε_1, ε_∞, f_1 and f_2 are obtained from equations (8), (9), (10), (12), and (13), and σ'_{eff} and σ''_{eff} are:

$$\sigma'_{eff} = (f_{\mathrm{GHz}}/1.35)\left(\frac{\sigma_1 - \sigma_2}{1+(f_{\mathrm{GHz}}/1.35)^2}\right) \tag{67}$$

$$\sigma''_{eff} = \sigma_2 + \frac{\sigma_1 - \sigma_2}{1+(f_{\mathrm{GHz}}/1.35)^2} \tag{68}$$

and

$$\sigma_1 = 0.0467 + 0.2204\,\rho_b - 0.004111 P_{sand} - 0.006614 P_{clay} \tag{69}$$

$$\sigma_2 = -1.645 + 1.939\,\rho_b - 0.0225622 P_{sand} + 0.01594 P_{clay} \tag{70}$$

The complex relative permittivity of two examples of soil types are shown in Figs 14, 15 and 16. The soil composition in Figs 14 and 16 are identical except for the volumetric water content, indicating that both the real part and imaginary part of the complex relative permittivity are directly related to the volumetric water content.

FIGURE 14

Complex relative permittivity of a silty loam soil as a function of frequency ($m_{\mathrm{v}} = 0.5$, T = 23 °C, $\rho_s = 2.59$, $\rho_b = 1.5750$ g cm^{-3})

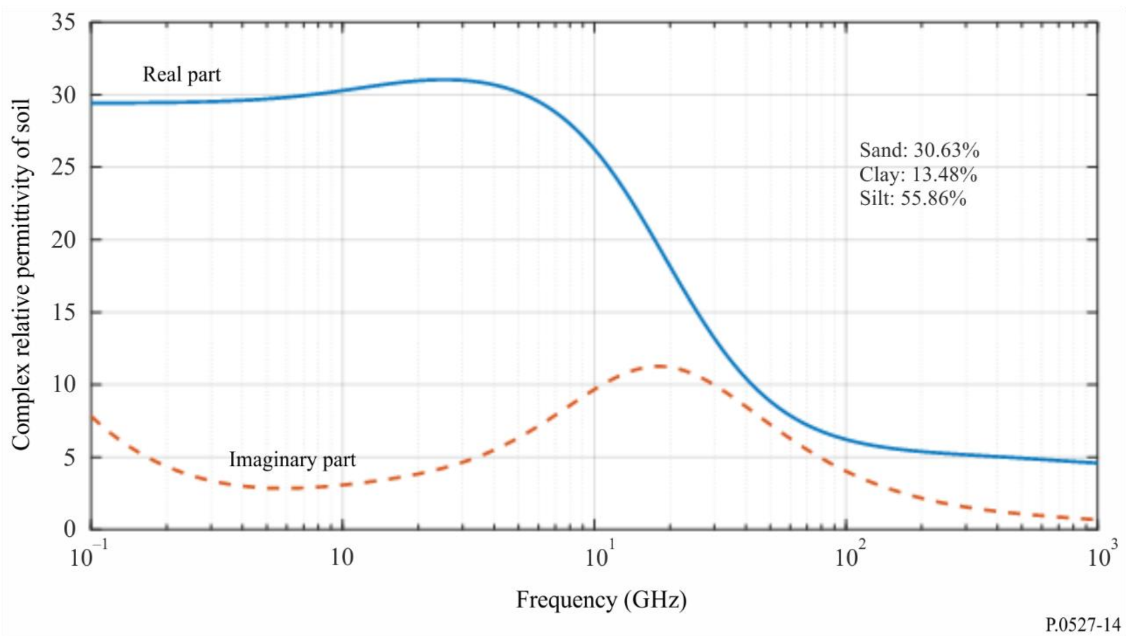

FIGURE 15

Complex relative permittivity of a silty clay soil as a function of frequency
(m_v= 0.5, T =23 °C, $\rho_s = 2.56$, $\rho_b = 1.4758$ g cm^{-3})

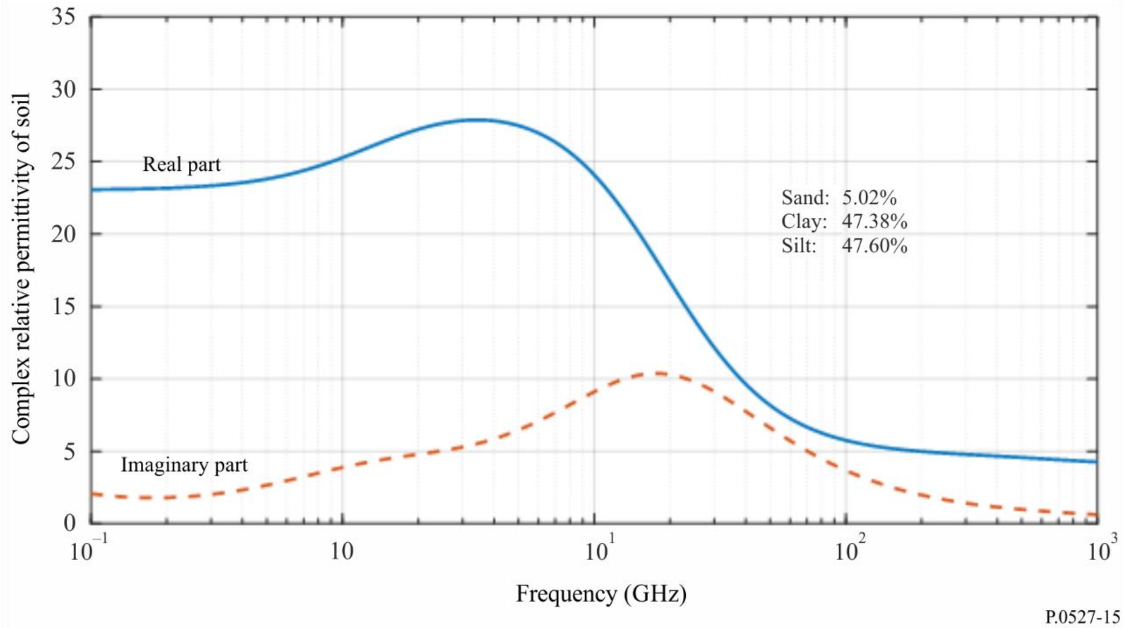

FIGURE 16

Complex relative permittivity of a silty loam soil as a function of frequency
(m_v= 0.07, T =23 °C, $\rho_s = 2.59$, $\rho_b = 1.5750$ g cm^{-3})

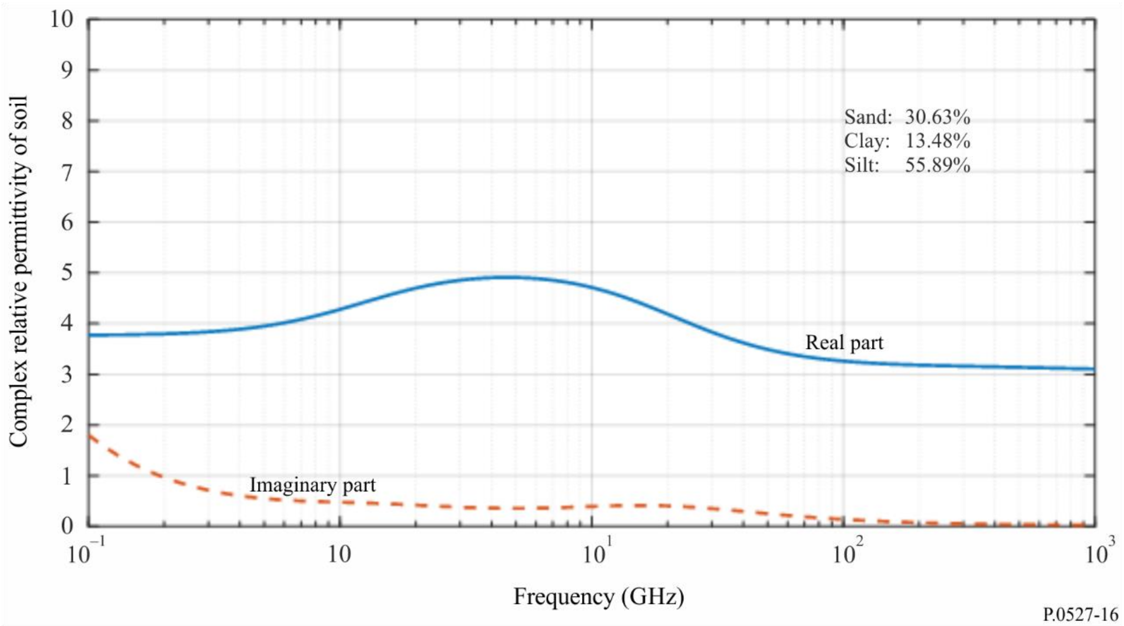

5.3 Vegetation

The complex relative permittivity of vegetation is a function of frequency f_{GHz} (GHz), temperature T (°C), and vegetation gravimetric water content, M_g, which is defined as

$$M_g = \frac{M_{mv} - M_{dv}}{M_{mv}} \tag{71}$$

M_{mv} is the weight of the moist vegetation, and M_{dv} is the weight of the dry vegetation. M_g is between 0.0 and 0.7.

This prediction method considers the vegetation as a mixture of bulk vegetation, saline free water, bounded water, and ice (if applicable). The complex relative permittivity of this mixture is given by

$$\varepsilon_{\mathrm{v}} = \varepsilon'_{\mathrm{v}} - j\,\varepsilon''_{\mathrm{v}} \tag{72}$$

The real part, $\varepsilon'_{\mathrm{v}}$, and the imaginary part, $\varepsilon''_{\mathrm{v}}$, of the complex relative permittivity of vegetation are given in § 5.3.1 for above freezing temperatures, and in § 5.3.2 for below freezing temperatures.

5.3.1 Above freezing temperatures

At temperatures above freezing (T > 0 °C), the real, and imaginary parts of the complex relative permittivity of vegetation are:

$$\varepsilon'_{\mathrm{v}} = \varepsilon_{d\mathrm{v}} + \mathrm{v}_{fw}\left[\varepsilon_{\infty} + \frac{(\varepsilon_s - \varepsilon_1)}{1+(f_{\mathrm{GHz}}/f_1)^2} + \frac{(\varepsilon_1 - \varepsilon_{\infty})}{1+(f_{\mathrm{GHz}}/f_2)^2}\right] + \mathrm{v}_{bw}\left[2.9 + \frac{55\left[1+\sqrt{(f_{\mathrm{GHz}}/0.02f_1)}\right]}{1+2\sqrt{(f_{\mathrm{GHz}}/0.02f_1)}+(f_{\mathrm{GHz}}/0.01f_1)}\right] \tag{73}$$

$$\varepsilon''_{\mathrm{v}} = \mathrm{v}_{fw}\left[\frac{(f_{\mathrm{GHz}}/f_1)(\varepsilon_s - \varepsilon_1)}{1+(f_{\mathrm{GHz}}/f_1)^2} + \frac{(f_{\mathrm{GHz}}/f_2)(\varepsilon_1 - \varepsilon_{\infty})}{1+(f_{\mathrm{GHz}}/f_2)^2} + \frac{22.86}{f_{\mathrm{GHz}}}\right] + \mathrm{v}_{bw}\left[\frac{55\sqrt{(f_{\mathrm{GHz}}/0.02f_1)}}{1+2\sqrt{(f_{\mathrm{GHz}}/0.02f_1)}+(f_{\mathrm{GHz}}/0.01f_1)}\right] \tag{74}$$

where $\varepsilon_{d\mathrm{v}}$ is the real part of the relative permittivity of bulk vegetation, v_{fw} is the free water volume fraction, and v_{bw} is the bound water volume fraction with:

$$\varepsilon_{d\mathrm{v}} = 1.7 - 0.74\,M_g + 6.16M_g^2 \tag{75}$$

$$\mathrm{v}_{fw} = M_g(0.55\,M_g - 0.076) \tag{76}$$

$$\mathrm{v}_{bw} = 4.64M_g^2/\left(1 + 7.36M_g^2\right) \tag{77}$$

ε_s, ε_1, ε_{∞}, f_1 and f_2 are obtained from equations (8), (9), (10), (12) and (13) respectively.

Equations (73) and (74) are more general than equation (16) of Recommendation ITU-R P.833 since they account for both free and bound water and include the temperature dependence.

The real and imaginary parts of the complex relative permittivity of vegetation vs. frequency at two different values of gravimetric water content are shown in Figs 10 and 11 demonstrating that both the real part and the imaginary part of the complex relative permittivity of vegetation increase as the gravimetric water content increases.

FIGURE 17

Complex relative permittivity of vegetation as a function of frequency
($M_g = 0.68, T = 22$ °C)

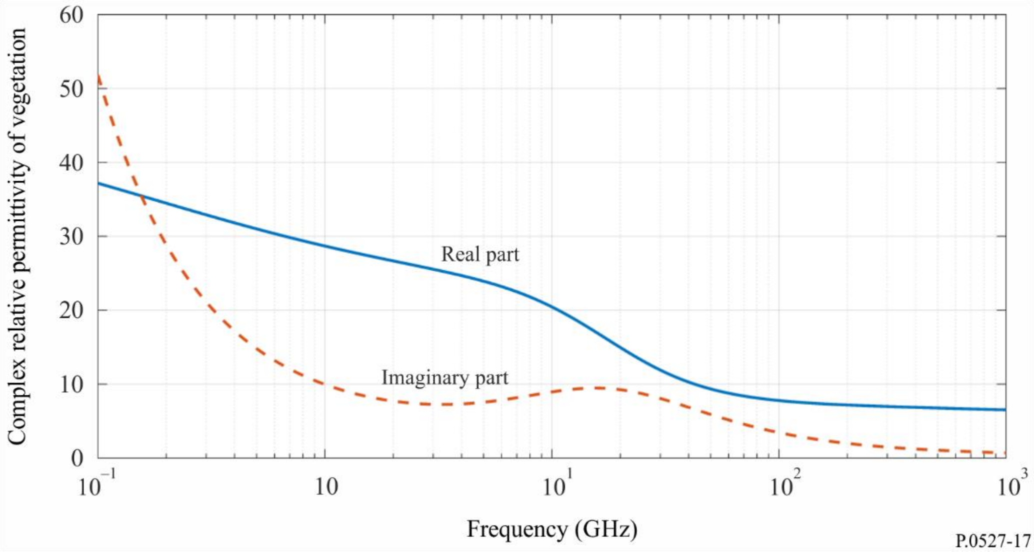

FIGURE 18

Complex relative permittivity of vegetation as a function of frequency
($M_g = 0.26, T = 22$ °C)

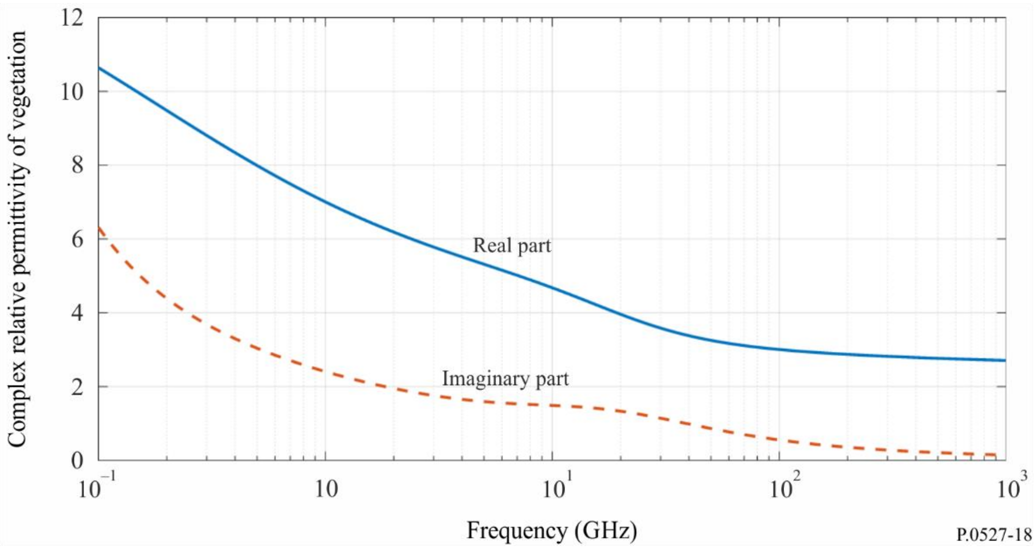

5.3.2 Below freezing temperatures

For below freezing temperatures between (−20 °C ≤ T < 0 °C) the real and imaginary parts of the complex relative permittivity are:

$$\varepsilon'_{\mathrm{v}} = \varepsilon_{dv} + \mathrm{v}_{fw}\left[4.9 + \frac{82.2}{1+(f_{\mathrm{GHz}}/9)^2}\right] + \mathrm{v}_{bw}[8.092 + 14.2067\,X1] + 3.15\,\mathrm{v}_{ice} \quad (78)$$

$$\varepsilon''_{\mathrm{v}} = \mathrm{v}_{fw}\left[\frac{82.2(f_{\mathrm{GHz}}/9)}{1+(f_{\mathrm{GHz}}/9)^2} + \frac{11.394}{f_{\mathrm{GHz}}}\right] + 14.2067\,\mathrm{v}_{bw}\,Y1 \quad (79)$$

where:

$$\varepsilon_{dv} = 6.76 - 10.24\,M_g + 6.19M_g^2 \quad (80)$$

$$\mathrm{v}_{fw} = \left(-0.106 + 0.6591M_g - 0.610M_g^2\right)\exp\left(\left(0.06 + 0.6883M_g + 0.0001M_g^2\right)\Delta\right) \quad (81)$$

$$\mathrm{v}_{bw} = \left(-0.16 + 1.1876M_g - 0.387M_g^2\right)\exp\left(\left(0.721 - 1.2733M_g + 0.8139M_g^2\right)\Delta\right) \quad (82)$$

$$\mathrm{v}_{ice} = A_{ice}\,\Delta^2 + B_{ice}\Delta + C_{ice} \quad (83)$$

$$A_{ice} = 0.001 - 0.012M_g + 0.0082M_g^2 \quad (84)$$

$$B_{ice} = 0.036 - 0.2389M_g + 0.1435M_g^2 \quad (85)$$

$$C_{ice} = -0.0538 + 0.4616M_g - 0.3398M_g^2 \quad (86)$$

$$\mathrm{X1} = \frac{1 + (f_{\mathrm{GHz}}/1.2582)^{0.2054}\cos(0.2054\pi/2)}{1 + 2\,(f_{\mathrm{GHz}}/1.2582)^{0.2054}\cos(0.2054\pi/2) + (f_{\mathrm{GHz}}/1.2582)^{0.4108}} \quad (87)$$

$$\mathrm{Y1} = \frac{(f_{\mathrm{GHz}}/1.2582)^{0.2054}\sin(0.2054\pi/2)}{1 + 2\,(f_{\mathrm{GHz}}/1.2582)^{0.2054}\cos(0.2054\pi/2) + (f_{\mathrm{GHz}}/1.2582)^{0.4108}} \quad (88)$$

$$\Delta = T - T_f \quad (89)$$

and the vegetation freezing temperature, T_f, is −6.5 ºC.

The real and the imaginary parts of the complex relative permittivity vs. frequency and temperature are shown in Figs 19 and 20. These Figures show that reducing the temperature below freezing decreases both the real and imaginary parts of the vegetation complex relative permittivity, and decreases the dependence of those parameters on frequency. For frequencies above 20 GHz, the complex relative permittivity of vegetation becomes less dependent on temperature.

FIGURE 19

Complex relative permittivity of vegetation as a function of frequency
($M_g = 0.68, T = -7$ ºC)

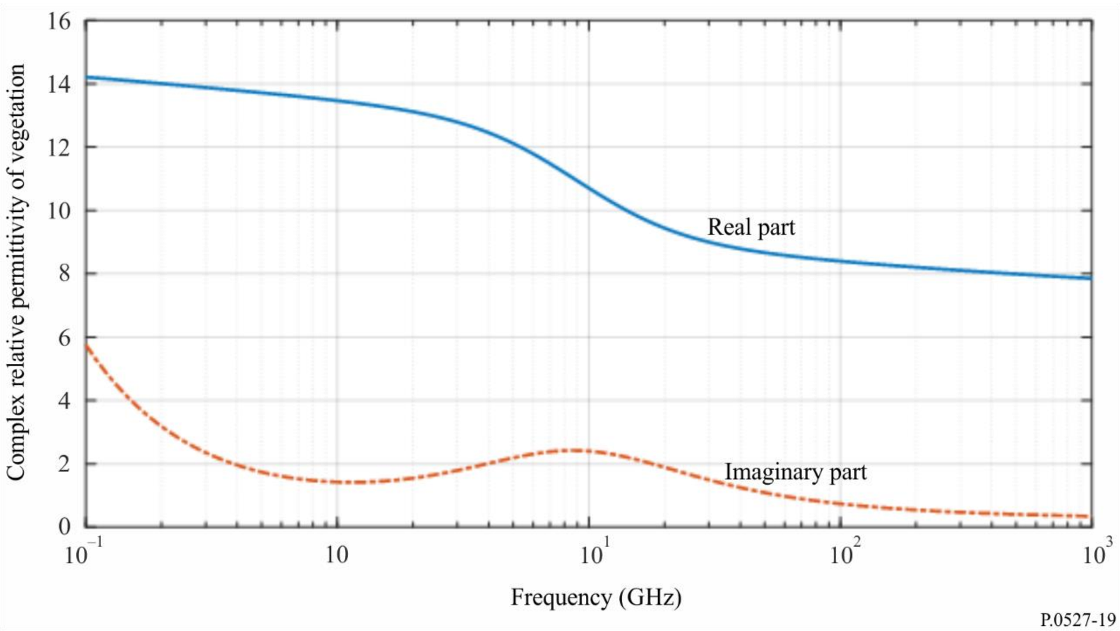

P.0527-19

FIGURE 20

Complex relative permittivity of vegetation as a function of frequency
($M_g = 0.68, T = -10$ °C)

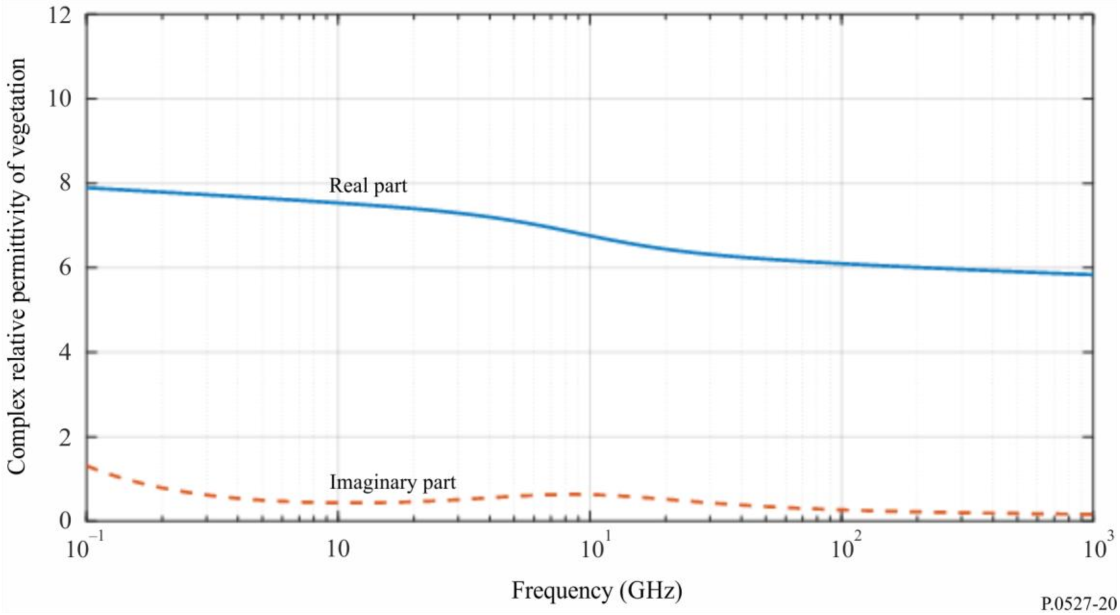

6 Emissivity

Emissivity, ϵ, is defined as the ratio of the energy radiated from a material's surface to the energy radiated from a perfect blackbody emitter at the same temperature, frequency, and viewing conditions. Emissivity and reflectivity, ρ, at the same frequency are related by the conservation of energy; i.e. $\epsilon + \rho = 1$. The emissivity of a surface is related to its complex relative permittivity, ε, via the Fresnel equations:

$$\epsilon = 1 - \left|r_p\right|^2, \quad p = v, h, c \tag{90}$$

where:

$$r_v = \frac{\varepsilon\cos\theta - \sqrt{\varepsilon - \sin^2\theta}}{\varepsilon\cos\theta + \sqrt{\varepsilon - \sin^2\theta}} \tag{91}$$

$$r_h = \frac{\cos\theta - \sqrt{\varepsilon - \sin^2\theta}}{\cos\theta + \sqrt{\varepsilon - \sin^2\theta}} \tag{92}$$

$$r_c = \frac{r_v + r_h}{2} \tag{93}$$

The subscript $p = h$ is for the horizontally polarized component and $p = v$ is for the vertically polarized component, and the subscript $p = c$ is for circular polarization. θ is the angle between the incident wave and normal incidence (i.e. $\theta = 0°$ for normal incidence). For the special case of normal incidence,

$$r_v = \frac{\varepsilon - \sqrt{\varepsilon}}{\epsilon + \sqrt{\epsilon}} \tag{94}$$

$$r_h = \frac{1 - \sqrt{\varepsilon}}{1 + \sqrt{\varepsilon}} \tag{95}$$

in which case:

$$r_v = \frac{\varepsilon - \sqrt{\varepsilon}}{\varepsilon + \sqrt{\varepsilon}} = -\frac{\sqrt{\varepsilon}}{\sqrt{\varepsilon}}\,\frac{1 - \sqrt{\varepsilon}}{1 + \sqrt{\varepsilon}} = -\frac{1 - \sqrt{\varepsilon}}{1 + \sqrt{\varepsilon}} = -r_h \tag{96}$$

Then $r_c = 0$, and $\epsilon = 1$.

For normal incidence and the vertically and horizontally polarized components, the emissivity of sea water for a smooth and flat specular ocean surface corresponding to the conditions in Fig. 2 (i.e. $T = 20$ °C and $S = 35$ ppt) is shown in Fig. 21; the emissivity of silty clay soil corresponding to the conditions in Fig. 15 (i.e. $P_{Sand} = 5.02\%$, $P_{Clay} = 47.38\%$, $P_{Silt} = 47.60\%$, $m_v = 0.5$, $T = 23\ °C$, $\rho_s = 2.56$, $\rho_b = 1.4758$ g/cm^3) is shown in Fig. 22; and the emissivity of vegetation corresponding to the conditions in Fig. 18 (i.e. $T = 22$°C, $M_g = 0.26$) is shown in Fig. 23.

FIGURE 21

Emissivity of sea water for a perfectly smooth sea surface ($T = 20$ °C and $S = 35$ ppt)

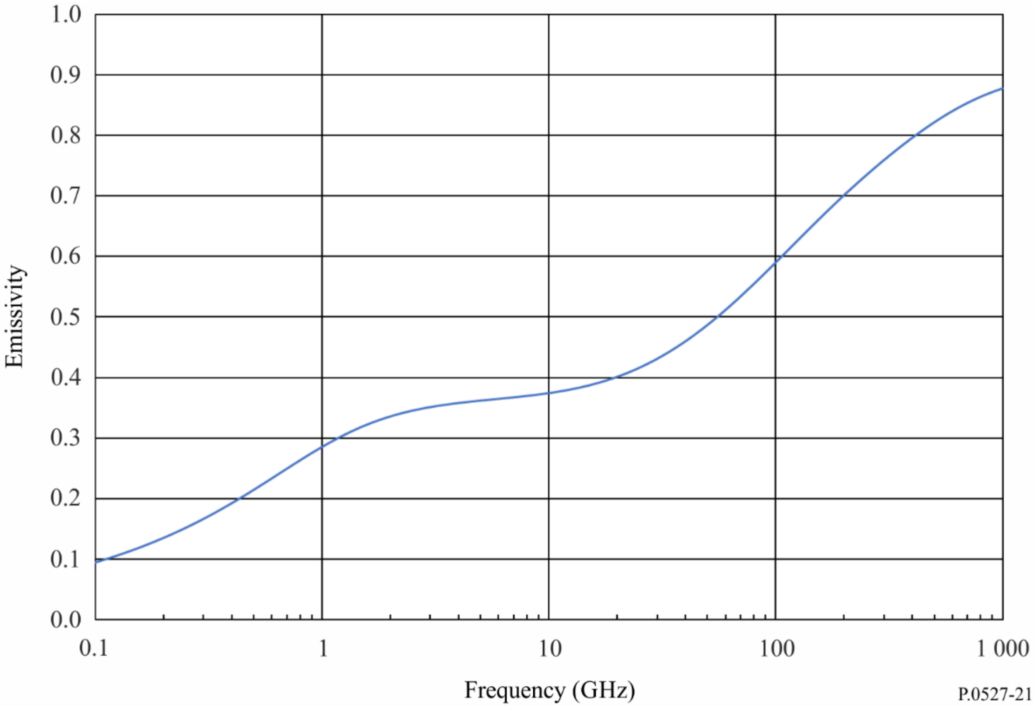

FIGURE 22

Emissivity of silty clay soil ($m_v = 0.5, T = 23$ °C, $\rho_s = 2.56$, $\rho_b = 1.4758\ g/cm^3$)

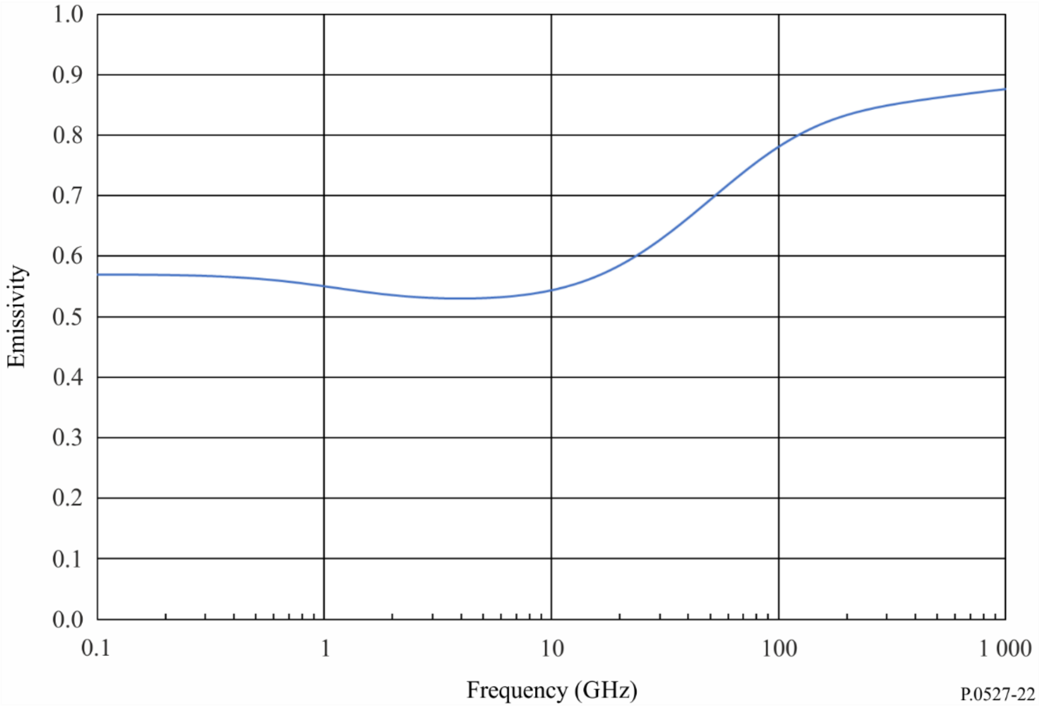

FIGURE 23

Emissivity of vegetation ($M_g = 0.26, T = 22$ °C)

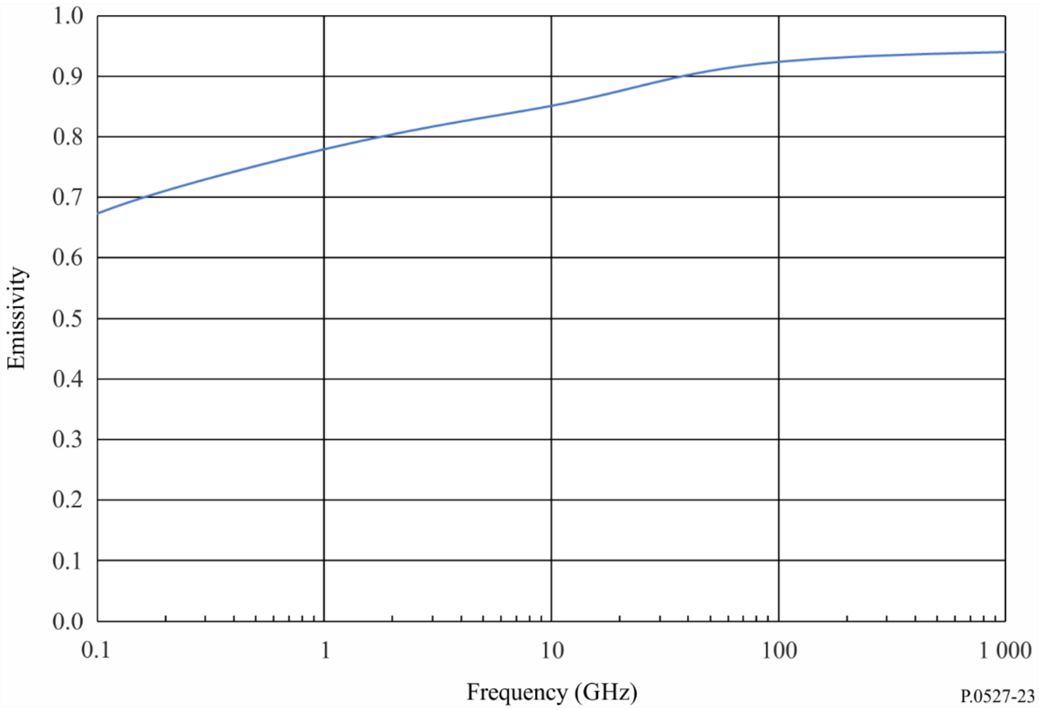

7 Isotropic emissivity of the ocean

The isotropic emissivity of the ocean, ϵ_{ocean}, is a function of polarization, frequency, incidence angle, wind speed, temperature, and salinity and is well-approximated by:

$$\epsilon_{ocean}(p, f_{GHz}, \theta, W, T, S) = \epsilon_{ocean,0}(p, f_{GHz}, \theta, T, S) + \Delta\epsilon_{\text{ocean}}(p, f_{\text{GHz}}, \theta, W, T, S)$$

where $\epsilon_{ocean,0}(p, f_{GHz}, \theta, T, S)$ is the emissivity, ϵ, in § 6 using the complex permittivity of sea water, ε_{sw}, in § 5.1.2; and $\Delta\epsilon_{\mathrm{ocean}}(p, f_{\mathrm{GHz}}, \theta, W, T, S)$ is the incremental isotropic emissivity as a function of wind speed. The parameters are:

p: polarization (v = vertical; h = horizonal)

f_{GHz}: frequency (GHz)

θ: incidence angle

W: wind speed (m/s)

T: ocean-surface temperature (°C)

S: salinity (ppt)

and

$$\Delta\epsilon_{\mathrm{ocean}}(p, f_{\mathrm{GHz}}\theta, W, T, S) = \widehat{\Delta}\epsilon_{ocean}(p, f_{GHz}, \theta_{ref}, W, T, S)\left(\frac{\theta}{\theta_{ref}}\right)^{x_p} + \frac{1}{2}\left[\widehat{\Delta}\epsilon_{\mathrm{ocean}}(v, f_{GHz}, \theta_{ref}, W, T, S) + \widehat{\Delta}\epsilon_{ocean}(h, f_{GHz}, \theta_{ref}, W, T, S)\right] \times \left[1 - \left(\frac{\theta}{\theta_{ref}}\right)^{x_p}\right] \quad (97)$$

where $x_v = 4.0$, $x_h = 1.5$,

$$\widehat{\Delta}\epsilon_{ocean}(p, f_{GHz}, \theta_{ref}, W, T, S) = \delta_{ref}(p, f_{GHz}, W)\,\frac{\epsilon_{ocean,0}(p, f_{GHz}, \theta_{ref}, T, S)}{\epsilon_{ocean,0}(p, f_{GHz}, \theta_{ref}, T_{ref}, S)} \quad (98)$$

where $\theta_{ref} = 55.2°$, $T_{ref} = 20°\mathrm{C}$,

$$\delta_{ref}(p, f_{GHz}, W) = \sum_{k=1}^{5} \delta_k(p, f_{GHz})\, W^k \quad (99)$$

and the coefficients $\delta_k(p, f_{GHz})$ are given in Table 3.

This model is valid from 6.8 to 85.5 GHz and for Earth incidence angles between 0 and 65 degrees (i.e. elevation angles between 25 and 90 degrees). For wind speeds above 20 m/s (i.e. 72 km/h), the emissivity should be calculated by linearly extrapolating the emissivity at a wind speed of 20 m/s. Emissivities at frequencies between the frequencies listed in Table 3 can be calculated by linearly interpolating the emissivity between the frequencies in Table 3.

TABLE 3

$\delta_k(p, f_{GHz})$ coefficients

f_{GHz} (GHz)	p	δ_1	δ_2	δ_3	δ_4	δ_5
6.8	v	4.96726E-05	−3.03363E-04	5.60506E-05	−2.86408E-06	4.88803E-08
6.8	h	3.85750E-03	−5.10844E-04	4.89469E-05	−1.50552E-06	1.20306E-08
10.7	v	−2.35464E-04	−2.76866E-04	5.73583E-05	−2.94364E-06	4.89421E-08
10.7	h	4.17650E-03	−6.20751E-04	6.82607E-05	−2.47982E-06	2.80155E-08
18.7	v	3.26502E-05	−3.65935E-04	6.62807E-05	−3.40705E-06	5.81231E-08
18.7	h	5.06330E-03	−7.41324E-04	8.54446E-05	−3.28225E-06	4.01950E-08
37.0	v	−7.03594E-04	−2.17673E-04	4.00659E-05	−1.84769E-06	2.76830E-08
37.0	h	5.63832E-03	−8.43744E-04	1.06734E-04	−4.61253E-06	6.67315E-08
85.5	v	−3.14175E-03	4.06967E-04	−3.33273E-05	1.26520E-06	−1.67503E-08
85.5	h	6.01311E-03	−7.00158E-04	1.26075E-04	−7.27339E-06	1.35737E-07

Attachment
to Annex 1

Electrical properties expressed as permittivity and conductivity as used in Recommendations ITU-R P.368 and ITU-R P.832

1 Introduction

Figure 24 below is reproduced from Fig. 1 of Recommendation ITU-R P.527-3, showing typical values of conductivity and permittivity for different types of ground, as a function of frequency. These graphs are retained from earlier revisions of this Recommendation as a convenience to users of Recommendations ITU-R P.368 and ITU-R P.832.

FIGURE 24

Relative permittivity ε_r, and conductivity σ, as a function of frequency